THE JOURNAL OF BIOLOGICAL CHEMISTRY VOL. 287, NO. 9, pp. 6912–6927, February 24, 2012
Published in the U.S.A.

Tannic Acid Is a Natural β-Secretase Inhibitor That Prevents Cognitive Impairment and Mitigates Alzheimer-like Pathology in Transgenic Mice*

Received for publication, August 15, 2011, and in revised form, December 20, 2011 Published, JBC Papers in Press, January 4, 2012, DOI 10.1074/jbc.M111.294025

Takashi Mori,[a,b1] Kavon Rezai-Zadeh,[c] Naoki Koyama,[a] Gary W. Arendash,[d,e] Haruyasu Yamaguchi,[f] Nobuto Kakuda,[g] Yuko Horikoshi-Sakuraba,[g] Jun Tan,[h,i] and Terrence Town[c,j,k2]

From the Departments of [a]Biomedical Sciences and [b]Pathology, Saitama Medical Center and University, Kawagoe, Saitama 350-8550, Japan, the [c]Department of Biomedical Sciences and Regenerative Medicine Institute Neural Program and the [j]Department of Neurosurgery, Maxine Dunitz Neurosurgical Institute, Cedars-Sinai Medical Center, Los Angeles, California 90048, the [d]Florida Alzheimer's Disease Research Center and the [e]Department of Cell Biology, Microbiology, and Molecular Biology, University of South Florida, Tampa, Florida 33620, the [f]Gunma University School of Health Sciences, Maebashi, Gunma 371-8514, Japan, the [g]Immuno-Biological Laboratories Co., Ltd., Fujioka, Gunma 375-0005, Japan, the [h]Rashid Laboratory for Developmental Neurobiology, Silver Child Development Center and the [i]Neuroimmunology Laboratory, the Department of Psychiatry and Neurosciences, College of Medicine, University of South Florida, Tampa, Florida 33613, and the [k]Department of Medicine, David Geffen School of Medicine, University of California, Los Angeles, California 90048

Background: Recent focus has been given to anti-amyloidogenic naturally occurring polyphenols known as flavonoids.
Results: The polyphenol tannic acid prevented behavioral impairment and mitigated Alzheimer disease-like pathology.
Conclusion: Tannic acid may be prophylactic for Alzheimer disease by inhibiting β-secretase activity and mitigating brain pathology.
Significance: This nutraceutical approach offers a new class of drug for inhibiting β-secretase with few if any side effects.

Amyloid precursor protein (APP) proteolysis is essential for production of amyloid-β (Aβ) peptides that form β-amyloid plaques in brains of Alzheimer disease (AD) patients. Recent focus has been directed toward a group of naturally occurring anti-amyloidogenic polyphenols known as flavonoids. We orally administered the flavonoid tannic acid (TA) to the transgenic PSAPP mouse model of cerebral amyloidosis (bearing mutant human APP and presenilin-1 transgenes) and evaluated cognitive function and AD-like pathology. Consumption of TA for 6 months prevented transgene-associated behavioral impairment including hyperactivity, decreased object recognition, and defective spatial reference memory, but did not alter nontransgenic mouse behavior. Accordingly, brain parenchymal and cerebral vascular β-amyloid deposits and abundance of various Aβ species including oligomers were mitigated in TA-treated PSAPP mice. These effects occurred with decreased cleavage of the β-carboxyl-terminal APP fragment, lowered soluble APP-β production, reduced β-site APP cleaving enzyme 1 protein stability and activity, and attenuated neuroinflammation. As *in vitro* validation, we treated well characterized mutant human APP-overexpressing murine neuron-like cells with TA and found significantly reduced Aβ production associated with less amyloidogenic APP proteolysis. Taken together, these results raise the possibility that dietary supplementation with TA may be prophylactic for AD by inhibiting β-secretase activity and neuroinflammation and thereby mitigating AD pathology.

Alzheimer disease (AD)[3] is the most common dementia and is a growing worldwide public health concern (1). AD neuropathological hallmarks include extracellular deposits of amyloid-β (Aβ) peptides, intracellular neurofibrillary tangles, neuronal and synaptic degeneration/loss, and neuroinflammation (2). Brain Aβ deposition likely results from increased peptide accumulation/reduced clearance, endorsing toxic events that drive AD pathogenesis (3, 4). Aβ is produced from sequential endoproteolytic cleavage of amyloid precursor protein (APP) by β- and γ-secretases (5–9), and enters a dynamic equilibrium between soluble and deposited forms (10). In recent years, much attention has been directed toward soluble multimeric forms of Aβ peptides as the toxic species. These so-called "Aβ oligomers" disrupt synaptic function and induce neurotoxicity *in vivo* (11–13).

* This work was supported, in whole or in part, by National Institutes of Health Grants 5R00AG029726-04, 3R00AG029726-04S1, and 1R01NS076794-01 from the NIA and the NINDS (to T. T.), Grant-in-aid for Scientific Research (C) 22500320 (to T. M.) from the Japan Society for the Promotion of Science and Grant-in-aid for Scientific Research (B) 19300122 (to H. Y.) from the Ministry of Education, Culture, Sports, Science and Technology, Alzheimer's Association Zenith Fellows Award ZEN-10-174633 (to T. T.), and American Federation of Aging Research/Ellison Medical Foundation Julie Martin Mid-Career Award in Aging Research M11472 (to T. T.).

[1] To whom correspondence may be addressed. Tel.: 81-49-228-3592; E-mail: t_mori@saitama-med.ac.jp.

[2] Inaugural holder of the Ben Winters Endowed Chair in Regenerative Medicine. To whom correspondence may be addressed: Regenerative Medicine Institute, Cedars-Sinai Medical Center, 8700 Beverly Blvd., Steven Spielberg Building, Rm. 361, Los Angeles, CA 90048. Tel.: 310-248-8581; E-mail: terrence.town@cshs.org.

[3] The abbreviations used are: AD, Alzheimer disease; CTF, carboxyl-terminal fragment; APP, amyloid precursor protein; Aβ, amyloid-β; BACE1, β-site APP cleaving enzyme 1; CAA, cerebral amyloid angiopathy; EGCG, (−)-epigallocatechin-3-gallate; TA, tannic acid; Iba1, ionized calcium-binding adapter molecule 1; GFAP, glial fibrillary acidic protein; QPCR, quantitative real-time PCR; ANOVA, analysis of variance; CC, cingulate cortex; H, hippocampus; EC, entorhinal cortex; sAPP, soluble APP.

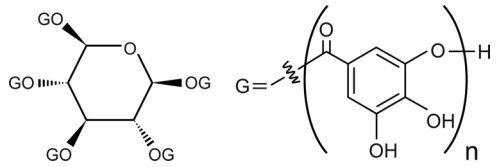

FIGURE 1. **Chemical structure of tannic acid (CAS 1401–55-4, $C_{76}H_{52}O_{46}$).** TA consists of a glucose core, which covalently connects to 3–5 gallic acid (3,4,5-trihydroxyl benzoic acid) residues through ester bonds. Each gallate residue can covalently link to other gallic acid molecules. Thus, TA is referred to as a glucoside polymer of gallic acid.

Rooted in the "amyloid cascade hypothesis" of AD, which purports that cerebral Aβ accumulation sets a toxic downstream cascade into motion (2–4), much focus has been directed toward anti-amyloid therapies. Specific approaches include reducing cerebral Aβ production or enhancing Aβ clearance (14–19). Although synthetic drugs have been anti-amyloid agents of choice, these compounds can have significant undesirable side effects, especially when given long-term in a disease prevention paradigm. For example, the ADAPT trial to test nonsteroidal anti-inflammatory drugs for primary AD prevention was prematurely halted due to nonsteroidal anti-inflammatory drug-associated cardiotoxicity (20, 21). Naturally occurring dietary compounds, or "nutraceuticals," represent an alternative class of molecules that typically have fewer side effects than designer drugs (22).

Others and we have previously reported that nutraceuticals including the green tea polyphenol (−)-epigallocatechin-3-gallate (EGCG) (23, 24), the citrus bioflavonoid luteolin (25), grape-derived polyphenols (26, 27), and caffeine (28) have anti-amyloidogenic properties. Based on our findings that EGCG enhances α-secretase APP cleavage and mitigates cerebral amyloidosis in the Tg2576 mouse model of cerebral amyloidosis (23, 24), we sought to investigate a structurally related compound, tannic acid (TA). TA is a plant-derived hydrolyzable tannin polyphenol (29) that is a gallic acid polymer glucoside ($C_{76}H_{52}O_{46}$; Fig. 1). In addition to structural similarity between TA and EGCG (both contain gallate moieties), both compounds inhibit/destabilize Aβ fibrils *in vitro* (30–32). To explore whether TA impacted AD-like features, we orally administered the compound for 6 months to the doubly transgenic (APP + $PS1_{\Delta E9}$) PSAPP mouse model of cerebral amyloidosis and examined behavioral impairment, AD-like pathology, APP processing, and neuroinflammation. Additionally, we validated our results *in vitro* using mutant human APP-overexpressing murine neuron-like cells.

EXPERIMENTAL PROCEDURES

Mice—Male double transgenic "Swedish" $APP_{K670N/M671L}$ (APPswe) plus Presenilin 1 exon 9 deleted ($PS1_{\Delta E9}$) B6C3-Tg 85Dbo/J mice on a C57BL/6xC3H background (designated PSAPP mice) were obtained from the Jackson Laboratory (Bar Harbor, ME) and were bred with female C57BL/6 mice to yield mutant PSAPP (APPswe + $PS1_{\Delta E9}$) and wild-type (WT) offspring. PSAPP mice overproduce human $A\beta_{1-40}$ and $A\beta_{1-42}$ peptides and develop progressive cerebral β-amyloid deposits and learning and memory impairment (33–36). All mice were characterized by PCR genotyping for mutant human APP and PS1 transgenes as described elsewhere (35). We strictly used PSAPP and WT littermates obtained from this breeding strategy for all analyses. Thus, all mice used in this study are genetically comparable.

TA was obtained from Sigma, resuspended in distilled water, and orally administered to 16 PSAPP mice (PSAPP-TA mice; 8 males and 8 females). As a vehicle control, 16 additional PSAPP mice received distilled water (PSAPP-V mice; 8 males and 8 females). In addition, 32 WT littermates received TA (WT-TA mice; 8 males and 8 females) or distilled water (WT-V mice, 8 males and 8 females). Beginning at 6 months of age, animals were gavaged with TA (30 mg/kg) or vehicle once daily for 6 months. In parallel, to examine if PSAPP mice were cognitively impaired at the initiation of dosing and whether TA treatment prevented *versus* delayed kinetics of disease progression, 12 untreated PSAPP mice (PSAPP-6M, 6 males and 6 females) and 12 untreated WT mice (WT-6M, 6 males and 6 females) at 6 months of age were included for analyses of behavior, β-amyloid pathology, and neuroinflammation. Mice were housed in a specific pathogen-free barrier facility under a 12/12-h light-dark cycle, with *ad libitum* access to food and water. All experiments were performed in accordance with the guidelines of the Animal Use Ethics Committee of the Saitama Medical University and of the NIH.

Behavioral Analyses—Two weeks prior to sacrifice, a battery of behavioral tests was conducted to assess exploratory activity, novel-object recognition and memory retention, and spatial learning and memory in the six groups of mice detailed above. Exploratory activity was evaluated by individually placing mice into a novel environment (the left corner of a white polyethylene chamber; $54 \times 39 \times 20$ cm). Their activity was recorded for 20 min by an overhead video camera (BL-C131, Panasonic, Fukuoka, Japan) connected to a Windows PC, and horizontal locomotion and rearing scores were counted for each 2-min time bin (37, 38). The next day, novel-object recognition and memory retention were assessed as described (39). Briefly, each mouse was habituated in a cage for 4 h, and then two different shaped objects were concurrently provided to the mouse for 10 min. The number of times that the mouse explored the object (defined as number of instances where a mouse directed its nose 2 cm or less distance from the object) that was later replaced by a novel object was counted for the initial 5 min of exposure (training phase). To test memory retention on the following day, one of the original objects was replaced with a different shaped novel object, and then the number of explorations of the novel object was counted for 5 min (retention test). The recognition index, taken as an index of memory, is reported as frequency (%) of explorations of the novel *versus* original objects.

Subsequently, Morris water maze testing was performed essentially as previously described (40, 41). The water maze consisted of a circular pool (80 cm diameter) filled with water maintained at 23–26 °C. For the purpose of post hoc analyses, the pool was divided into quadrants (Q1 to Q4), and a 6-cm diameter plexiglass platform was located 1 cm above the water surface in the center of Q2. After a minimum of 20 min habituation to the room, mice naïve to the test were placed in the pool and allowed to search for the platform for 60 s. On the first 2 days (four trials were conducted per day with a 20-min inter-

trial interval), a visible cue was placed on the platform and its location was randomly varied among four possible locations (counterbalanced across mice). The trial ended when a mouse climbed the platform, or in the allocated 60 s, whichever came first. After finding and climbing on the platform, each mouse was allowed to remain there for 20 s, and was then returned to its cage. Animals that did not locate the platform within 60 s were guided to it and allowed to remain there for 20 s before being returned to their cages. On the third day, submerged platform testing was conducted for five consecutive days (learning phase; four trials per day with a 20-min inter-trial interval). The location of the indiscernible platform remained in Q2, 1 cm below the water surface, and mice were placed into the pool in one of seven randomly selected locations (excluding the position immediately adjacent to the platform). One day after the conclusion of the learning phase, memory retention was determined in a single 60-s probe trial. The submerged platform was removed from the water maze, and mice were placed and released opposite the site where the platform had been located and time spent in each quadrant was recorded for the probe trial. All behavioral tests were performed in a room (6 m × 4.5 m) with indirect lighting and multiple visible cues on the walls. The examiner determined the time of swimming until the mouse reached the platform (latency) using a stopwatch. In addition, trials were recorded using an overhead video camera and were analyzed using customized macro software in Microsoft Excel. All trials were performed at the same time of day (±1 h), during the animals' light phase. So as not to interfere with behavioral testing, TA or vehicle treatment was carried out 1 h after behavioral testing.

Tissue Preparation—Tissue was processed according to our previously described methods (16, 18, 42, 43). At 12 months of age, animals were anesthetized with sodium pentobarbital (50 mg/kg) and euthanized by transcardial perfusion with ice-cold physiological saline containing heparin (10 units/ml). Brains were isolated and quartered (sagittally at the level of the longitudinal fissure of the cerebrum, and then coronally at the level of the anterior commissure) using a mouse brain slicer (Muromachi Kikai, Tokyo, Japan). Right anterior cerebral quarters were weighed and snap-frozen at −80 °C for α- or β-secretase activity analyses. Right posterior cerebral quarters were further divided into two pieces, and weighed and snap-frozen at −80 °C. One-half was sequentially extracted in Tris-buffered saline (TBS; 25 mM Tris-HCl, pH 7.4, 150 mM NaCl), 2% SDS-, and guanidine-soluble fractions for Aβ sandwich enzyme-linked immunosorbent assays (ELISAs). The other half was used for holo-APP, β-site APP cleaving enzyme 1 (BACE1), and β-carboxyl-terminal fragment (β-CTF: phospho-C99 and C99) Western blots. Left anterior cerebral quarters were weighed and immersed in RNA stabilization solution (RNAlater®, Applied Biosystems, Foster City, CA) and then snap-frozen at −80 °C for proinflammatory cytokine and BACE1 quantitative real-time PCR (QPCR) analyses. Left posterior cerebral quarters were immersion fixed in 4% paraformaldehyde in 0.1 M phosphate buffer at 4 °C overnight, and routinely processed in paraffin for immunohistochemical analyses.

Immunohistochemistry—For paraffin blocks, we sectioned five coronal sections (per set) with a 100 μm interval and a thickness of 5 μm for each brain region (for cingulate cortex (CC), bregma −0.10 to −0.82 mm; for hippocampus (H) and entorhinal cortex (EC), bregma −2.92 to −3.64 mm) (44). We prepared three sets of five sections in each separate region for analyses of Aβ deposits/β-amyloid plaques (for burden, plaque number, and maximum diameter morphometry) as well as ionized calcium-binding adapter molecule 1 (Iba1, to mark reactive microglia) and glial fibrillary acidic protein (GFAP, an astrocytosis marker) burdens. Immunohistochemical staining was conducted according to the manufacturer's protocol using a Vectastain ABC *Elite* kit (Vector Laboratories, Burlingame, CA) coupled with the diaminobenzidine reaction, except that the biotinylated secondary antibody step was omitted for Aβ immunohistochemical staining. The following primary antibodies were used: a biotinylated human Aβ monoclonal antibody (4G8; 1:200, Covance Research Products, Emeryville, CA), Iba1 polyclonal antibody (1:1,000, Wako, Osaka, Japan), and GFAP polyclonal antibody (1:500, Dako, Carpinteria, CA). Using additional sets of five sections, normal mouse or rabbit serum (isotype control) or phosphate-buffered saline (0.1 M PBS, pH 7.4) was used instead of primary or secondary antibody or ABC reagent as negative controls.

Image Analysis—Quantitative image analysis was done based on previously validated methods (16, 18, 42, 43). Images were acquired as digitized tagged-image format files to retain maximum resolution using a BX60 microscope with an attached CCD camera system (DP-70, Olympus, Tokyo, Japan), and digital images were routed into a Windows PC for quantitative analyses using SimplePCI software (Hamamatsu Photonics, Hamamatsu, Shizuoka, Japan). We captured images of five 5-μm sections through each anatomic region of interest (CC, EC, and H) based on anatomical criteria defined by Franklin and Paxinos (44), and obtained a threshold optical density that discriminated staining from background. Each anatomic region of interest was manually edited to eliminate artifacts. For Aβ, Iba1 (microgliosis), and GFAP (astrocytosis) burden analyses, data are reported as the percentage of labeled area captured (positive pixels) divided by the full area captured (total pixels). Selection bias was controlled for by analyzing each region of interest in its entirety.

For β-amyloid plaque morphometric analyses, diameters (based on maximum length) of β-amyloid plaques were measured, and numbers of β-amyloid plaques falling into three mutually exclusive diameter categories (<25, 25–50, or >50 μm) were tabulated. Results are presented as mean plaque number per mouse in each region examined. For cerebral amyloid angiopathy (CAA) morphometric analysis, we counted numbers of Aβ antibody-stained cerebral vessels in each anatomic region of interest based on our previous methods (43); those data are shown as mean CAA deposit number per mouse.

Cell Culture—The N2a cell line that stably overexpresses human "Swedish"-mutated APP-695 (SweAPP N2a cells) was kindly provided by Dr. Gopal Thinakaran (Department of Neurobiology, University of Chicago). SweAPP N2a cells were grown in Dulbecco's modified Eagle's medium supplemented with 10% fetal calf serum, 2 mM glutamine, 100 units/ml of penicillin, 0.1 μg/ml of streptomycin, and 200 μg/ml of G418 sulfate according to previously described methods (16, 23, 25).

SweAPP N2a cells were seeded in 24-well tissue culture plates at 1×10^5 cells per well. Cultured cells were differentiated into neuron-like cells by 2 h pre-treatment with neurobasal media containing 300 μM dibutyryl cAMP and then treated with TA (1.563, 3.125, 6.25, 12.5, or 25 μM) or 0.1 M PBS (pH 7.4; as vehicle control) for 12 h in the same media prior to analyses.

Lactate Dehydrogenase Release Assay—SweAPP N2a cells were seeded in 24-well tissue culture plates at 1×10^5 cells per well. Culture cells were differentiated into neuron-like cells by 2 h pre-treatment with neurobasal media containing 300 μM dibutyryl cAMP and then treated with TA (3.125, 6.25, 12.5, or 25 μM) or 0.1 M PBS (pH 7.4; vehicle control) for 12 h in the same media. Culture wells were then assayed for cell death by a lactate dehydrogenase release assay (Promega) as described (45).

Cell-free BACE1 Activity Assay—To directly test the effect of TA on BACE1 activity, we used available kits based on secretase-specific peptides conjugated to DABCYL/EDANS fluorogenic reporter molecules (Cayman Chemical, Ann Arbor, MI) in accordance with the manufacturer's instructions. Briefly, BACE1 enzyme was incubated with various concentrations of TA (1.563, 3.125, 6.25, 12.5, or 25 μM) or BACE1 inhibitor II (1.25 μm; as a positive control) in the presence of 1× reaction buffer for 40 min prior to reading fluorescence values on a FLUOstar Omega (BMG LABTECH, San Diego, CA) fluorescent microplate reader.

ELISA—We separately quantified $A\beta_{1-40}$ and $A\beta_{1-42}$ in brain homogenates and cultured SweAPP N2a cell supernatants by sandwich ELISAs. Brain $A\beta_{1-40}$ and $A\beta_{1-42}$ species were detected by a three-step extraction protocol according to previously published methods (46, 47). Briefly, we homogenized brains using TissueLyser LT (Qiagen, Valencia, CA; two times for 1 min at 50 Hz) in TBS solution containing protease inhibitor mixture (Sigma), centrifuged homogenates at 18,800 × *g* for 60 min at 4 °C, and removed the supernatants (TBS-soluble fraction). Resulting pellets were treated with 2% SDS in H_2O with the same protease inhibitors and homogenized using TissueLyser LT (one time for 1 min at 50 Hz). We then centrifuged the homogenates at 18,800 × *g* for 60 min at 4 °C and collected supernatants (2% SDS-soluble fraction). Finally, the remaining pellets were treated with 5 M guanidine HCl and dissolved by occasional mixing on ice for 30 min, then centrifuged at 18,800 × *g* for 60 min at 4 °C, and supernatants were collected representing the guanidine HCl-soluble fraction.

$A\beta_{1-40}$ and $A\beta_{1-42}$ species were separately quantified in individual samples in duplicate using ELISA kits (catalogue number 27718 for $A\beta_{1-40}$ and number 27712 for $A\beta_{1-42}$; IBL, Fujioka, Gunma, Japan) in accordance with the manufacturer's instructions (48). We also quantified Aβ oligomers in the 2% SDS-soluble fraction in duplicate individual samples by Aβ oligomer ELISA (catalogue number 27725; IBL) according to the manufacturer's instructions (49). All samples fell within the linear range of the standard curve. $A\beta_{1-40}$ and $A\beta_{1-42}$ ELISA values are reported as picograms of $A\beta_{1-x}$/wet mg of brain, and the Aβ oligomer concentration is reported as picomolar.

Western Blot—Cultured SweAPP N2a cells were treated with various doses of TA (1.563, 3.125, 6.25, 12.5, or 25 μM) or 0.1 M PBS (pH 7.4; as a vehicle control) for 12 h. Cultured cells were then lysed in ice-cold lysis buffer (containing 20 mM Tris-HCl, pH 7.5, 150 mM NaCl, 1 mM Na_2EDTA, 1 mM EGTA, 1% Triton X-100, 2.5 mM sodium pyrophosphate, 1 mM β-glycerophosphate, 1 mM Na_3VO_4, 1 μg/ml of leupeptin, and 1 mM PMSF). Mouse brain homogenates were lysed in TBS solution containing protease inhibitor mixture (Sigma) followed by TNE buffer (10 mM Tris-HCl, 1% NP-40, 1 mM EDTA, and 150 mM NaCl), and aliquots corresponding to 10 μg of total protein were electrophoretically separated using 10 or 15% Tris glycine gels based on target protein molecular weights. Electrophoresed proteins were transferred to polyvinylidene difluoride membranes (Bio-Rad) that were subsequently blocked in blocking buffer (1% (w/v) nonfat dry milk in TBS containing 0.1% (v/v) Tween 20) for 1 h at ambient temperature. After blocking, membranes were hybridized for 1 h at ambient temperature with primary antibodies: amino-terminal APP polyclonal antibody (1:400, IBL), carboxyl-terminal soluble APP-α (sAPP-α) monoclonal antibody (2B3; 1:100, IBL) directed against amino acids DAEFRHDSGYEVHHQK, carboxyl-terminal soluble APP-β (sAPP-β) monoclonal antibody that recognizes Swedish mutant (ISEVNL) protein (6A1; 1:100, IBL), carboxyl-terminal BACE1 polyclonal antibody (1:400, IBL), amino-terminal Aβ monoclonal antibody (82E1; 1:150, IBL), carboxyl-terminal APP polyclonal antibody (1:1,000, Merck Millipore, Billerica, MA), or actin polyclonal antibody as a loading control (1:500, Santa Cruz Biotechnology, Santa Cruz, CA). Membranes were then rinsed three times for 30 min each in TBS containing 0.1% (v/v) Tween 20 and incubated for 1 h at ambient temperature with appropriate horseradish peroxidase-conjugated secondary antibodies. After additional rinsing as above, membranes were incubated for 5 min at ambient temperature with enhanced chemiluminescence substrate (SuperSignal West Dura Extended Duration Substrate, Thermo Fisher Scientific, Waltham, MA), exposed to film, and developed.

Secretase Activity Assays—For α- and β-secretase activity analyses in brain homogenates, we used available kits based on secretase-specific peptides conjugated to fluorogenic reporter molecules (DABCYL/EDANS; R & D Systems, Minneapolis, MN) according to our published methods (23, 43). Briefly, brains were lysed in ice-cold 1× cell extraction buffer for 10 min and centrifuged at 18,800 × *g* for 1 min. Supernatants were collected and kept on ice. Appropriate amounts of brain homogenate, reaction buffer, and fluorogenic substrate were added in duplicate to a 96-well plate and incubated in the dark at 37 °C for various periods of time. Following incubation, fluorescence was monitored (335 nm excitation and 495 nm emission) at 25 °C using a SH-9000 microplate fluorimeter with SF6 software (CORONA ELECTRIC, Hitachinaka, Ibaraki, Japan). Background was determined from negative controls (omission of brain homogenate or fluorogenic substrate).

QPCR—We quantified tumor necrosis factor-α (TNF-α), interleukin-1β (IL-1β), BACE1, and β-actin mRNA levels by QPCR. Total RNA was extracted using the RNeasy Mini Kit (Qiagen), and first strand cDNA synthesis was carried out using the QuantiTect Reverse Transcription Kit (Qiagen) in accordance with the manufacturer's instructions. We diluted cDNA 1:1 in H_2O and carried out QPCR for all genes of interest using

cDNA-specific TaqMan primer/probe sets (TaqMan Gene Expression Assays, Applied Biosystems) on an ABI 7500 Fast Real-time PCR instrument (Applied Biosystems). Each 20-μl reaction mixture contained 2 μl of cDNA with 1 μl of TaqMan Gene Expression Assay reagent, 10 μl of TaqMan Fast Universal PCR Master Mix (Applied Biosystems), and 7 μl of H_2O. Thermocycler conditions consisted of: 95 °C for 15 s, followed by 40 cycles of 95 °C for 1 s and 60 °C for 20 s. TaqMan probe/primer sets were as follows: mouse TNF-α (catalogue number Mm00443258_m1), mouse IL-1β (number Mm00434228_m1), mouse BACE1 (number Mm00478664_m1), and mouse β-actin (number Mm00607939_s1; used as an internal reference control) (Applied Biosystems). Samples that were not subjected to reverse transcription were run in parallel as negative controls to rule out genomic DNA contamination (data not shown). A "no template control" was also included for each primer set (data not shown). The cycle threshold number (C_T) method (50) was used to determine relative amounts of initial target cDNA in each sample. Results for BACE1 expression are expressed relative to vehicle-treated WT mice, whereas TNF-α and IL-1β expression values are normalized to WT-6M littermates.

Statistical Analysis—All experiments were performed by an examiner blinded to sample identities, and code was not broken until the analyses were completed. Data are presented as the mean ± 1 S.E. A hierarchical analysis strategy was used for time-dependent behavioral data in which the first step was a repeated-measures analysis of variance (ANOVA) to assess the significance of the main effects and interactive terms. If significant, post hoc testing was done with Tukey's HSD or Dunnett's T3 methods, and appropriate p values are reported based on adjustment according to Levene's test for equality of the variance. For all other data, in instances of single mean comparisons, Levene's test followed by t test for independent samples was performed. In instances of multiple mean comparisons, one-way ANOVA was used, followed by post hoc comparison of the means using Bonferroni's or Dunnett's T3 methods (where appropriateness was determined using Levene's test). A p value of less than 0.05 was considered to be significant. All analyses were performed using the Statistical Package for the Social Sciences, release IBM SPSS 19.0 (IBM, Armonk, NY).

RESULTS

Oral Tannic Acid Treatment Mitigates Hyperactivity and Cognitive Impairment in PSAPP Mice—We began by orally administering TA or vehicle to PSAPP or WT mice starting at 6 months of age for a period of 6 months and subsequently conducted a behavioral testing battery. In addition, to examine cognitive status when dosing started, untreated PSAPP and WT mice at 6 months of age were included for analyses of behavior. When placed into a novel environment, PSAPP-V mice were hyperactive as measured by higher locomotion and rearing scores compared with the other 5 groups of mice (Fig. 2*A*). This behavioral phenotype has been observed in mouse models of cerebral amyloidosis (*e.g.* Tg2576 or PSAPP) (18, 34, 51), and may be associated with disinhibition resulting from cortical and/or hippocampal injury (38). Overall ANOVA showed main effects of time ($p < 0.001$), genotype ($p < 0.001$), and treatment ($p < 0.001$), and post hoc comparisons showed statistically significant differences between PSAPP-V mice and the other 5 mouse groups at each time point for locomotion scores (Fig. 2*A*, *, $p < 0.05$ for PSAPP-V *versus* PSAPP-TA, WT-V, WT-TA, PSAPP-6M, or WT-6M mice) and for rearing scores (Fig. 2*A*, *, $p < 0.05$ for PSAPP-V *versus* PSAPP-TA, WT-V, WT-TA, PSAPP-6M, or WT-6M mice). Hyperactivity was fully prevented in PSAPP-TA mice, as they did not statistically differ from WT-V WT-TA, PSAPP-6M, or WT-6M mice ($p > 0.05$).

We then tested learning and memory in the same cohort of mice by a novel object recognition assay. If mice remember an initial encounter with a novel object, they tend to preferentially explore the new *versus* familiar object, typically operationalized as "recognition index" (39). Although all groups performed similarly during the training phase of the test, in the retention phase, one-way ANOVA followed by post hoc comparison showed statistically significant differences on recognition index between PSAPP-V mice and the other 5 mouse groups as indicated (Fig. 2*B*, *, $p < 0.05$ for PSAPP-V *versus* PSAPP-TA, WT-V, WT-TA, PSAPP-6M, or WT-6M mice). Importantly, PSAPP-TA mice had significantly increased novel object exploration frequency *versus* PSAPP-V animals (Fig. 2*B*), but did not significantly differ from WT-V, WT-TA, PSAPP-6M, or WT-6M groups ($p > 0.05$), showing that TA also prevented novel object recognition impairment associated with PSAPP transgene expression.

We further tested animals in the Morris water maze, a widely accepted assay of spatial reference learning and memory in rodents (40, 41). For the learning phase of the test, overall ANOVA showed main effects of time ($p < 0.001$) and genotype ($p < 0.001$), and post hoc comparison revealed statistically significant differences between PSAPP-V mice and the other 5 mouse groups as indicated (Fig. 2*C*, *, $p < 0.05$ for PSAPP-V *versus* PSAPP-TA, WT-V, WT-TA, PSAPP-6M, or WT-6M mice). PSAPP-V mice had greater latency to reach the platform location after training than the other 5 mouse groups, whereas PSAPP-TA mice showed significant improvement, indicating that oral TA treatment inhibited PSAPP transgene-associated impaired spatial reference learning. For the probe trial (day 6 of testing), the invisible platform was removed from the pool and platform location memory was evaluated. When considering Q2 (goal quadrant) data, one-way ANOVA and post hoc testing showed statistically significant differences between PSAPP-V mice and the other 5 mouse groups as indicated (Fig. 2*D*, *, $p < 0.05$ for PSAPP-V *versus* PSAPP-TA, WT-V, WT-TA, PSAPP-6M, or WT-6M mice). PSAPP-TA mice swam in the goal quadrant significant longer than PSAPP-V mice, and their behavior did not significantly differ from WT-V, WT-TA, PSAPP-6M, or WT-6M mice, showing that TA treatment prevents PSAPP transgene-associated spatial memory impairment.

It is unlikely that behavioral differences in the Morris water maze were due to motivational issues or to locomotor impairment, as there were no significant between group differences ($p > 0.05$) on swim speed during either the learning or probe trial phases of the test. Moreover, it is important to note that the degree of thigmotaxis could indicate levels of anxiety and impact interpretation of Morris water maze results. In this regard, we did not observe evidence of thigmotaxis, operationalized as prolonged movement of the mice along the pool cir-

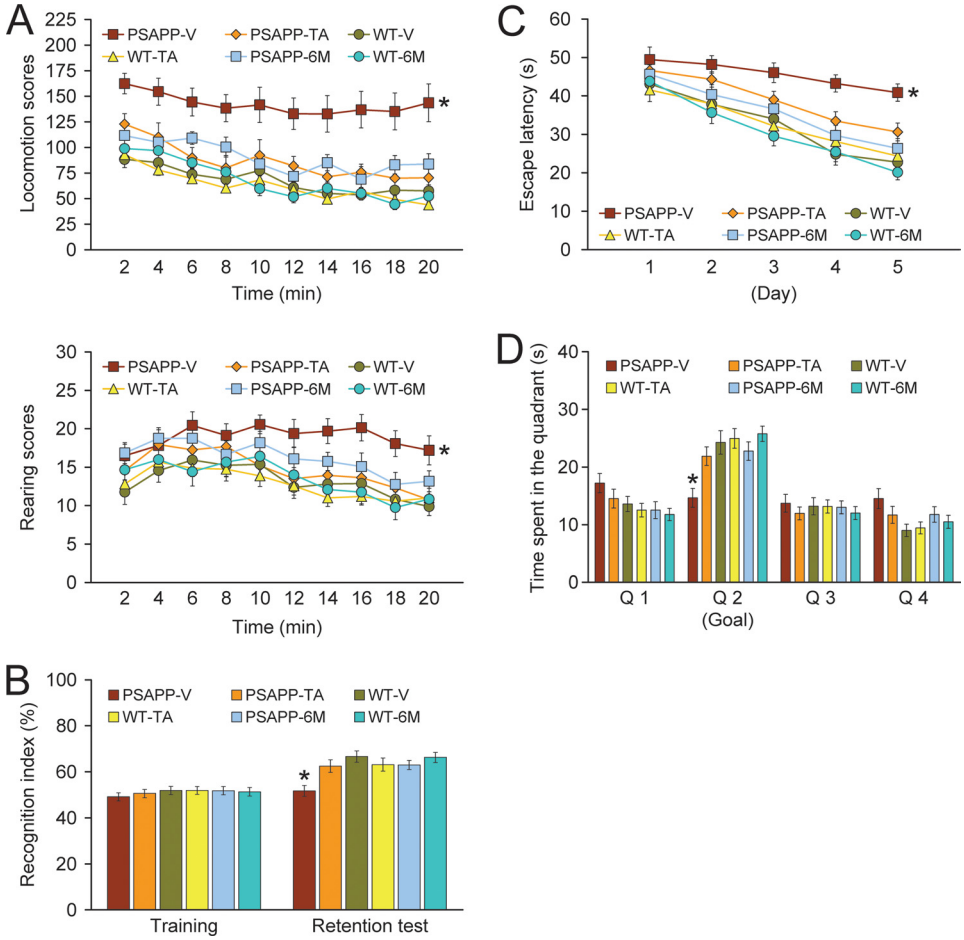

FIGURE 2. **Tannic acid treatment prevents behavioral impairment in PSAPP mice.** PSAPP mice received oral vehicle (*PSAPP-V*, $n = 16$) or TA (*PSAPP-TA*, $n = 16$) treatment, and wild-type mice were given vehicle (*WT-V*, $n = 16$) or TA (*WT-TA*, $n = 16$) orally for 6 months beginning at 6 months of age, and subjected to behavioral testing at 12 months of age. To examine cognitive status when dosing started, untreated 6-month-old PSAPP mice (*PSAPP-6M*, $n = 12$) and WT mice (*WT-6M*, $n = 12$) were included in the behavioral analyses. *A*, locomotion and rearing scores obtained from open field activity testing are shown. *B*, recognition index (%) in the object recognition test is shown (*left*, training phase; *right*, retention test phase). *C*, Morris water maze test data are shown from the submerged platform (learning phase) and from *D*, a single 60-s probe trial test (conducted 1 day after termination of the learning phase). All statistical comparisons are *versus* PSAPP-V mice.

cumference, in any mice examined during either the learning or probe trial phases of the test. Furthermore, untreated PSAPP mice at 6 months of age (PSAPP-6M) did not clearly show cognitive impairment as compared with WT mice at the same age or to WT-V or WT-TA mice at 12 months of age by open field, object recognition, or either the learning or probe trial phases of Morris water maze testing. Importantly, behavioral testing performance in PSAPP-TA mice was not significantly different from PSAPP-6M animals in each of the tests conducted. This result can be interpreted as prevention of cognitive impairment in PSAPP mice by a 6-month treatment regimen of TA. Finally, for all of the behavioral tests conducted, we used multiple ANOVA models with gender as a categorical covariate, but did not detect significant gender main effects or interactive terms ($p > 0.05$). We also stratified by gender and found a similar pattern of results as above in both males and females (data not shown).

Tannic Acid Treatment Ameliorates Aβ Pathology in an Accelerated Mouse Model of Cerebral Amyloidosis—We next evaluated Aβ/β-amyloid pathology by three strategies: Aβ antibody immunoreactivity (conventional β-amyloid "burden" analysis), β-amyloid morphometric analysis, and separate $A\beta_{1-40}$ and $A\beta_{1-42}$ sandwich ELISAs. PSAPP-V mice showed typical β-amyloid deposition (33, 36), which was significantly reduced by 51–58% in CC, EC, and H regions of PSAPP-TA mouse brains (Fig. 3, *A* and *B*, ***, $p < 0.001$). Of note, PSAPP-TA plaques were not completely attenuated *versus* PSAPP-6M mice (Fig. 3, *A* and *B*), indicating that TA mitigated as opposed to completely prevented cerebral amyloid deposition. TA reduction in β-amyloid deposits was independent of gender, being evident in both male and female PSAPP-TA *versus* PSAPP-V mice (data not shown). To assess whether reduced β-amyloid burden was specific to a particular plaque size subset or occurred more generally, we performed morphometric analysis of β-amyloid plaques in PSAPP-V and PSAPP-TA mice. According to previously described methods (18, 16, 42, 43), plaques were assigned to one of three mutually exclusive categories according to maximum diameter: small (< 25 μm), medium (between 25 and 50 μm), or large (>50 μm). Data showed that all three subsets of plaques were significantly reduced in PSAPP-TA *versus* PSAPP-V mice across all three brain regions examined (Fig. 3, *A* and *C*, ***, $p < 0.001$, % reduc-

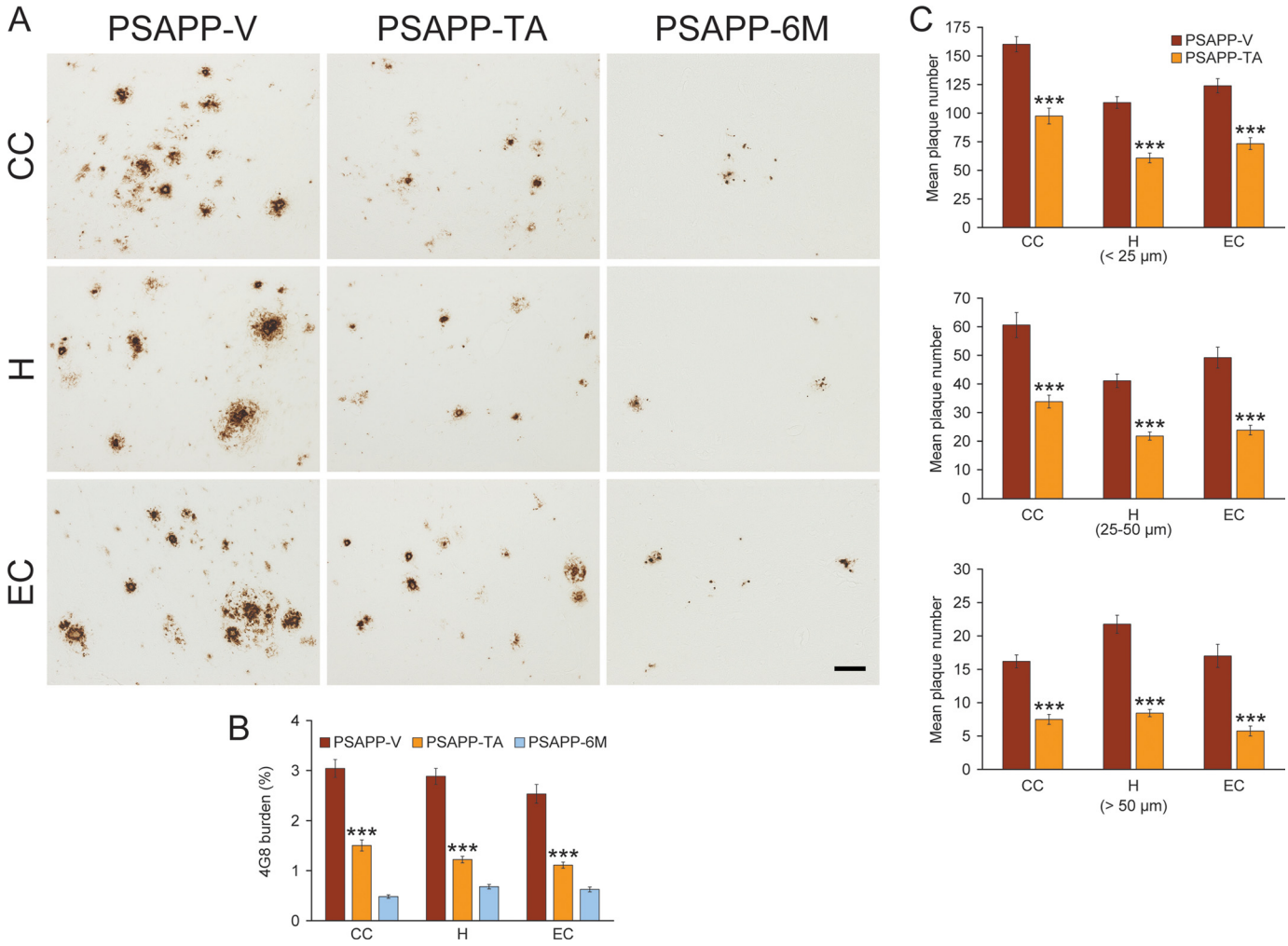

FIGURE 3. **Cerebral parenchymal β-amyloid deposits are mitigated in tannic acid-treated PSAPP mice.** Data were obtained from PSAPP mice treated with vehicle (*PSAPP-V*, $n = 16$) or TA (*PSAPP-TA*, $n = 16$) for 6 months commencing at 6 months of age (mouse age = 12 months at sacrifice). To examine if the TA treatment delayed *versus* prevented disease progression, untreated PSAPP mice (*PSAPP-6M*, $n = 12$) at 6 months of age were also included in these analyses. *A,* representative photomicrographs of 4G8 immunohistochemistry are shown for cerebral β-amyloid plaques in PSAPP-V, PSAPP-TA, and PSAPP-6M mice. Brain regions shown include: cingulate cortex (*CC*, *top*), hippocampus (*H*, *middle*), and entorhinal cortex (*EC*, *bottom*). *Scale bar* denotes 50 μm. *B*, quantitative image analysis for Aβ (4G8) burden is shown, and each brain region is indicated on the *x* axis. *C,* morphometric analysis of cerebral parencymal β-amyloid plaques is shown in PSAPP-V and PSAPP-TA mice. Brain sections were stained with 4G8 antibody, and plaques were counted based on maximum diameter and assigned to one of three mutually exclusive categories: small (<25 μm; *top*), medium (between 25 and 50 μm; *middle*), or large (>50 μm; *bottom*). Mean plaque subset number per mouse is shown on the *y* axis, and each brain region is represented on the *x* axis. The statistical comparison for *B* is within the brain region and *versus* PSAPP-TA mice, and for *C*, between PSAPP-V and PSAPP-TA mice.

tion for: small, 39–44%; medium, 44–52%; large, 54–66% plaque subsets). We stratified by gender and observed the same pattern of results in both males and females (data not shown). Untreated PSAPP-6M mice had quantitatively minor (0.5–0.7%) cerebral β-amyloid burden (Fig. 3, *A* and *B*), and the majority of these deposits were seed-like dots <25 μm in size, with only a few plaques between 25 and 50 μm. Because of this, we were unable to perform morphometric analysis of Aβ deposits for the PSAPP-6M group.

In addition to brain parenchymal deposition of β-amyloid as senile plaques, 83% of AD patients present with β-amyloid deposits in cerebral vessels, known as CAA (52). PSAPP mice also develop vascular β-amyloid deposits with age (36), and we found almost no evidence for CAA in young PSAPP-6M mice (data not shown). Having shown that TA treatment led to reduced brain parenchymal β-amyloid plaques in PSAPP mice, we wondered if cerebral vascular β-amyloid deposits might also be altered. In both PSAPP mouse groups, cerebral vascular β-amyloid deposits were predominantly detected within penetrating arteries at the pial surface in CC and EC regions and within small arteries at the hippocampal fissure. We scored Aβ antibody (4G8)-stained cerebral vascular deposits in PSAPP-V and PSAPP-TA mice and found reductions in PSAPP-TA mouse brains that reached statistical significance in all three brain regions examined (Fig. 4, *A* and *B*, **, $p < 0.01$).

In agreement with histological observations, biochemical analysis of Aβ species in brain homogenates revealed significant reductions in TBS-soluble $A\beta_{1-40}$ and in both $A\beta_{1-40}$ and $A\beta_{1-42}$ abundance in the detergent-soluble fraction from PSAPP-TA *versus* PSAPP-V mice (Fig. 4*C*, 25–33% depending on the particular Aβ species; *, $p < 0.05$). Similarly, extraction of the insoluble pellet in guanidine HCl revealed significant reductions in PSAPP-TA mice for both $A\beta_{1-40}$ and $A\beta_{1-42}$ levels (27–28%) by biochemical analysis (Fig. 4*C*, ***, $p < 0.001$).

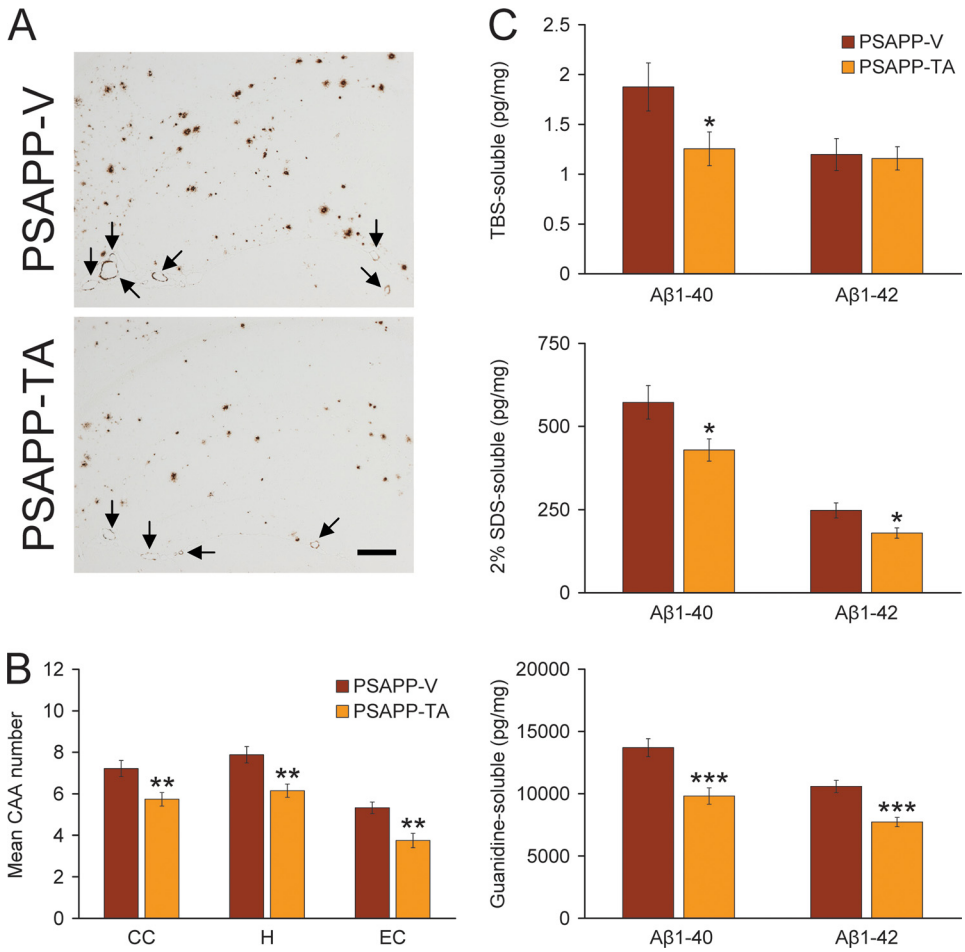

FIGURE 4. **Cerebral vascular β-amyloid deposits and brain Aβ levels are reduced in PSAPP mice given oral tannic acid treatment.** *A,* representative photomicrographs of 4G8 immunohistochemistry were taken from PSAPP-V and PSAPP-TA mouse hippocampi at 12 months of age, and cerebral vascular β-amyloid deposits are indicated (*arrows*). *Scale bar* denotes 200 μm. *B,* severity of cerebral amyloid angiopathy (mean CAA deposit number per mouse) is shown on the *y* axis with the brain region indicated on the *x* axis (*CC*, *H*, and *EC*). *C*, TBS-soluble, 2% SDS-soluble, and TBS-insoluble (but 5 M guanidine HCl-extractable) fractions from three-step extracted brain homogenates were examined by sandwich ELISA for human Aβ_{1-40} and Aβ_{1-42} levels. Data were obtained from PSAPP mice treated with vehicle (*PSAPP-V*, $n = 16$) or with TA (*PSAPP-TA*, $n = 16$) for 6 months commencing at 6 months of age. All statistical comparisons are within the brain region and/or between PSAPP-V and PSAPP-TA mice.

By contrast, Aβ_{1-42} levels in the TBS-soluble fraction were similar between PSAPP-TA and PSAPP-V mice. We also analyzed PSAPP-6M mice by Aβ biochemistry, but found low abundance of Aβ species that was below the threshold of ELISA detection in certain fractions (data not shown). Collectively, these data show that cerebral amyloidosis, including brain parenchymal and cerebral vascular β-amyloid deposits and Aβ peptide abundance, is delayed but not completely prevented by oral treatment with TA in PSAPP mice.

Inhibition of Cerebral Amyloidogenic APP Metabolism in Tannic Acid-treated PSAPP Mice—Mitigated cerebral amyloidosis in PSAPP-TA mice could be due to 1) increased brain-to-blood Aβ efflux (10), 2) reduced expression of APP or PS1 transgenes, or 3) attenuated amyloidogenic APP metabolism. We obtained peripheral blood samples from PSAPP-V and PSAPP-TA mice at the time of sacrifice and assayed plasma Aβ_{1-40} and Aβ_{1-42} species, but did not detect differences between groups (data not shown). To examine if TA-attenuated cerebral amyloidosis could be due to decreased expression of transgene-derived APP or PS1, we probed brain homogenates from PSAPP-V and PSAPP-TA mice using amino-terminal APP polyclonal or carboxyl-terminal PS1 monoclonal antibodies and found no change in APP or PS1 holoprotein levels (Fig. 5*A* and data not shown).

To determine whether APP metabolites including sAPP-α and sAPP-β were affected by TA treatment, brain homogenates were probed with monoclonal antibody 2B3 that detects the carboxyl terminus of human sAPP-α and with monoclonal antibody 6A1 that recognizes the carboxyl terminus of human Swedish mutant sAPP-β. Western blot and densitometry data showed significantly reduced expression of sAPP-β in PSAPP-TA mouse brains, whereas sAPP-α abundance did not differ between groups (Fig. 5, *A–C*, ***, $p < 0.001$). To further determine whether amyloidogenic APP processing was inhibited by TA treatment, we probed brain homogenates with a carboxyl-terminal BACE1 polyclonal antibody. Densitometry showed that BACE1 protein abundance was significantly decreased in PSAPP-TA mice (Fig. 5, *A* and *D*, *, $p < 0.05$). To assess whether this effect was due to TA attenuation of BACE1 transcription, relative expression levels of BACE1 mRNA were assayed in each mouse group by QPCR. However, there were no detectable differences between groups (Fig. 5*E*), suggesting a post-transcriptional mode of TA action on BACE1.

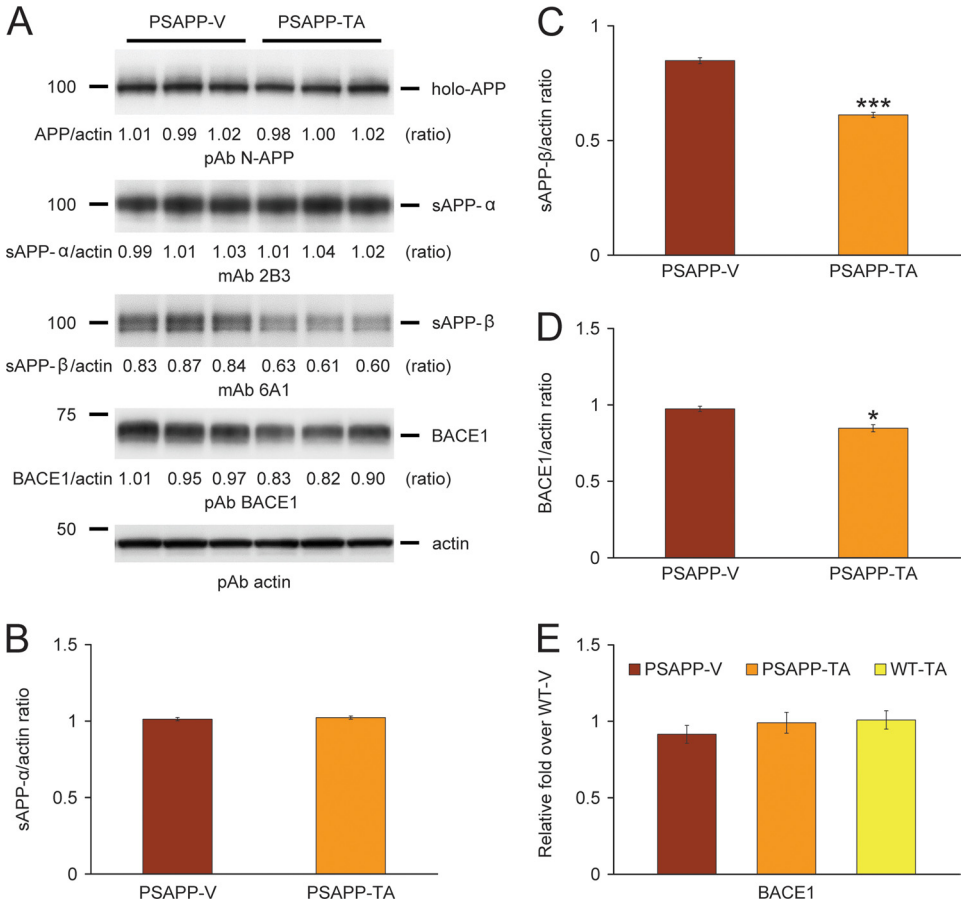

FIGURE 5. **Tannic acid inhibits BACE1 protein at the post-transcriptional level in PSAPP mice.** *A,* Western blots are shown using an amino (N)-terminal APP polyclonal antibody (*pAb N-APP*; holo-APP is shown), a carboxyl-terminal human sAPP-α monoclonal antibody (*mAb 2B3*; sAPP-α is shown), a carboxyl-terminal human sAPP-β monoclonal antibody (*mAb 6A1*; sAPP-β is shown), and a carboxyl-terminal β-site APP cleaving enzyme 1 polyclonal antibody (*pAb BACE1*). Actin is shown as a loading control for each blot. Densitometry analyses are shown for the ratio of: *B,* sAPP-α to actin; *C,* sAPP-β to actin; and *D,* BACE1 to actin. *E,* QPCR data reveal no differences between groups on BACE1 expression. Data are expressed as relative fold over WT-V mice. Data for *A–D* were obtained from PSAPP mice treated with vehicle (*PSAPP-V*, $n = 16$) or with TA (*PSAPP-TA*, $n = 16$) for 6 months beginning at 6 months of age. Wild-type mice treated with vehicle (*WT-V*, $n = 16$) or with TA (*WT-TA*, $n = 16$) were also included for *E*. The statistical comparisons for *C* and *D* are between PSAPP-V and PSAPP-TA mice.

To further address steady-state APP metabolism, we probed brain homogenates with monoclonal antibody 82E1 that recognizes amino acids 1–16 of human Aβ, and detects the amyloidogenic β-CTF (C-99) and phospho-β-CTF (P-C99) and monomeric plus oligomeric Aβ species. Densitometry confirmed that APP metabolism to phospho-C99 and C99 was significantly deceased in PSAPP-TA mice (Fig. 6, *A* and *B*, **, $p <$ 0.01). These effects were accompanied by reduced abundance of the Aβ species between 25 and 75 kDa (presumed Aβ oligomers) and monomeric Aβ in PSAPP-TA mice (Fig. 6*A*). To confirm that Aβ oligomers were attenuated by TA treatment, we quantified them in the detergent-soluble fraction by sandwich ELISA and found significant reduction in PSAPP-TA *versus* PSAPP-V mice (Fig. 6*C*, *, $p < 0.05$). Collectively, these data indicate that TA works at the protein level to inhibit BACE1 expression. Consistently, β-secretase activity was significantly decreased, whereas α-secretase activity was unaltered in brain homogenates from PSAPP-TA *versus* PSAPP-V mice (Fig. 6*D*, ***, $p < 0.001$ at each time point). These data support the notion that TA affords prophylaxis against cerebral amyloidosis by inhibiting amyloidogenic APP metabolism as a consequence of decreasing BACE1 expression at the protein (but not mRNA) level and reducing β-secretase activity.

Tannic Acid Reduces Aβ Production and Inhibits Amyloidogenic APP Metabolism in Neuron-like Cells—Mitigated cerebral amyloidosis and reduced amyloidogenic APP metabolism in PSAPP-TA mice could be due to a direct, neuron cell autonomous affect or to an indirect mode of TA action. To determine whether TA could directly modulate APP metabolism in neuron-like cells, we cultured SweAPP N2a cells, which stably express human APP bearing the Swedish mutation, and treated them with a dose-range of TA. As shown in Fig. 7*A*, TA dose dependently inhibited both $A\beta_{1-40}$ and $A\beta_{1-42}$ release into the media by separate sandwich ELISAs. Although the optimal effect occurred at 12.5 μM, significant reduction for both Aβ peptides was evident even at the lowest dose (3.125 μM) of TA used (*, $p < 0.05$; **, $p < 0.01$ for each dose *versus* PBS control).

We moved on to investigate whether these effects were because of reduced amyloidogenic APP metabolism, and performed Western blots with a carboxyl-terminal APP polyclonal antibody that simultaneously detects both amyloidogenic C99 and nonamyloidogenic C83 (α-carboxyl-terminal fragment, α-CTF) (Fig. 7*B*). Results qualitatively showed less abundance of C99 with increasing doses of TA. Quantitative densitometry followed by one-way ANOVA revealed a significant main effect of dose ($p < 0.01$), and post hoc testing revealed significant

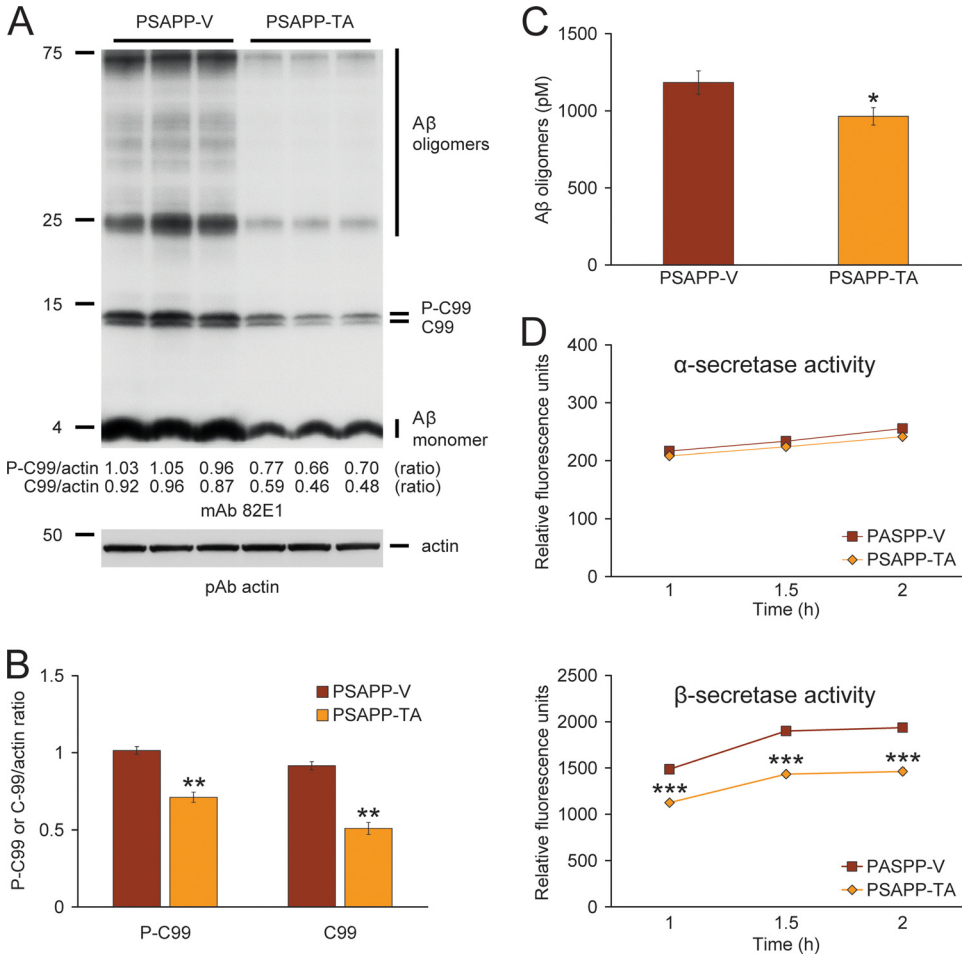

FIGURE 6. **Anti-amyloidogenic APP processing in PSAPP mice treated with tannic acid.** *A*, Western blots using an amino-terminal Aβ monoclonal antibody (*mAb 82E1*) are shown. This antibody detects various fragments generated by amyloidogenic APP cleavage, including: Aβ oligomers and monomer as well as phospho-C99 (*P-C99*) and non-phospho-C99 (*C99*). Actin is shown as a loading control. *B*, densitometry analysis is shown for ratios of C-99 or P-C99 to actin. *C*, the levels of Aβ oligomers in the 2% SDS-soluble brain homogenate fraction were measured by sandwich ELISA. *D*, α-secretase and β-secretase activity assays are shown. Relative fluorescence units are shown on the *y* axis, and reaction time is represented on the *x* axis. Data for *A–D* were obtained from PSAPP mice treated with vehicle (*PSAPP-V*, $n = 16$) or with TA (*PSAPP-TA*, $n = 16$) for 6 months beginning at 6 months of age. The statistical comparisons for *B–D* are between PSAPP-V and PSAPP-TA mice.

differences when comparing control (PBS-treated) SweAPP N2a cells to cells that were treated with 12.5 to 25 μM TA (Fig. 7*C*, *, $p < 0.05$). To determine whether BACE1 protein levels were reduced by TA treatment, we probed brain homogenates with a carboxyl-terminal BACE1 polyclonal antibody. Results showed TA dose-dependent inhibition of BACE1 protein (Fig. 7*D*).

To determine whether TA directly or indirectly inhibited BACE1 activity, we developed a BACE1 activity assay consisting of combining a dose range of TA in a cell-free system with BACE1 enzyme and fluorogenic reporters. The result was positive, as one-way ANOVA revealed a significant main effect of TA dose ($p < 0.001$) and post hoc testing revealed significant differences when comparing BACE1 enzyme alone (positive control) to samples that contained from 1.563 to 25 μM TA. Of note, significant reduction for BACE1 activity was evident even at the lowest dose (1.563 μm) of TA used (Fig. 7*E*, **, $p < 0.01$). BACE1 inhibitor II treatment (used as a BACE1 inhibitor control; $IC_{50} = 0.97$ μM) at 1.25 μM revealed an inhibitory effect for BACE1 (497.3 $\pm$ 8.8 relative fluorescence units) as compared with 100% BACE1 enzyme activity (646.3 $\pm$ 25.4 relative fluorescence units). Interestingly, this effect was quantitatively more minor than even the lowest dose of TA used in this system.

Finally, to determine whether escalating doses of TA were toxic to SweAPP N2a cells, we performed a lactate dehydrogenase release assay, but did not observe evidence of TA toxicity (Fig. 7*F*). When taken together, these data show that TA is capable of exerting a direct effect on reducing Aβ secretion and amyloidogenic APP metabolism in neuron-like cells.

Tannic Acid Attenuates Neuroinflammation in PSAPP Mice—Chronic activation of glial cells in and around β-amyloid plaques may be pathoetiologic in AD via production of numerous neurotoxic acute-phase reactants, proinflammatory cytokines, and immunostimulatory molecules (53, 54). Furthermore, neuroinflammation, as earmarked by β-amyloid plaque-associated reactive gliosis and increased expression of proinflammatory cytokines, has been demonstrated in aged transgenic mouse models of cerebral amyloid deposition (18, 42, 43, 55–57). To test whether TA impacted neuroinflammatory processes in PSAPP mice, we examined β-amyloid plaque-associated microgliosis (by Iba1 antibody) and astrocytosis (using GFAP antibody) immunoreactivity

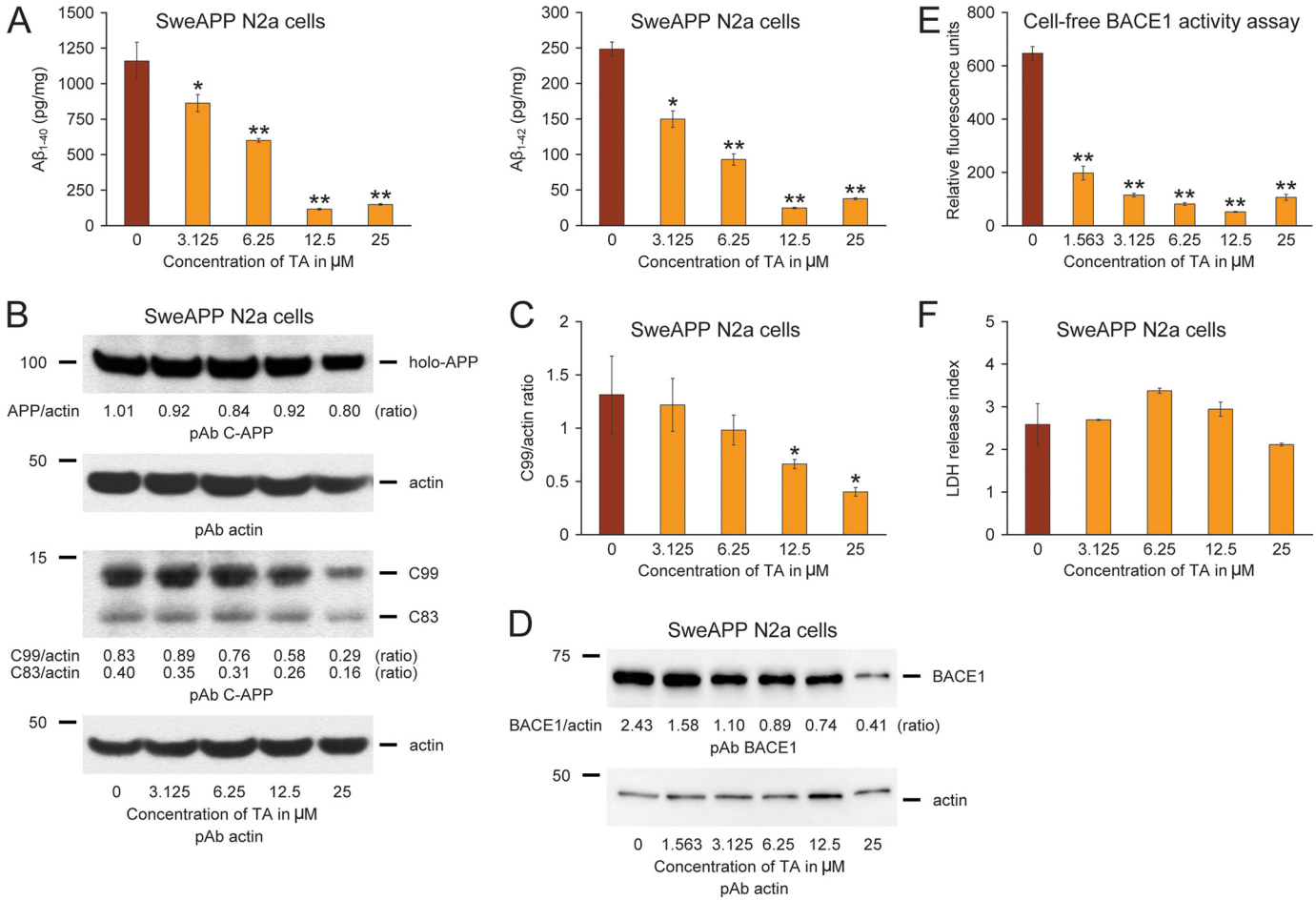

FIGURE 7. **Tannic acid reduces Aβ production and inhibits amyloidogenic APP metabolism in SweAPP N2a cells, and directly inhibits BACE1 in a cell-free system.** *A*, $A\beta_{1-40}$ and $A\beta_{1-42}$ species in cell supernatants from SweAPP N2a cells were separately measured by sandwich ELISA. *B*, promotion of anti-amyloidogenic APP processing in SweAPP N2a cells treated with TA. Western blots using a carboxyl-terminal APP polyclonal antibody (*pAb C-APP*) show holo-APP and carboxyl-terminal fragments generated by amyloidogenic APP cleavage (*C99*, β-CTF and *C83*, α-CTF). Actin is included as an internal reference control. *C*, densitometry analyses for the ratio of C99 to actin at various TA treatment doses are shown. *D*, BACE1 expression is inhibited in SweAPP N2a cells treated with TA. A representative pAb BACE1 Western blot is shown. Actin is included as an internal reference control, and ratiometric densitometry data are shown *below* each lane. *E*, cell-free BACE1 activity assay results are shown. Relative fluorescence units are shown on the *y* axis. *F*, lactate dehydrogenase (*LDH*) release assay for SweAPP N2a cells treated from 0 to 25 μM of TA. All statistical comparisons are *versus* 0 μM of TA, and similar results were observed in 2–3 independent experiments.

(conventional microgliosis and astrocytosis burden analyses) and quantified brain expression of the proinflammatory cytokines TNF-α and IL-1β. PSAPP-V mice demonstrated elevated β-amyloid plaque-associated reactive gliosis (microgliosis and astrocytosis), as evidenced by increased expression of Iba1 and GFAP in glial somata and processes. Yet, microgliosis and astrocytosis were significantly reduced in PSAPP-TA mice compared with PSAPP-V animals (Figs. 8, *A* and *B*, and 9, *A* and *B*, ***, $p < 0.001$). These effects were gender-independent, as a similar pattern of statistically significant results was observed in both male and female PSAPP-TA mice (data not shown). When considering brain mRNA abundance of TNF-α and IL-1β, a similar pattern of statistically significant results was found (Fig. 9*C*, **, $p < 0.01$). Neuroinflammation in PSAPP-TA mice was not reduced to levels of untreated PSAPP-6M mice, indicating mitigation but not complete prevention of this pathology (Figs. 8, *A* and *B*, and 9, *A–C*).

Phagocytic microglia have been detected in the aged APP23 cerebral amyloidosis mouse model in small numbers (58) and in increased abundance in aged Tg2576 mice bearing a CD11c promoter-driven dominant-negative transforming growth factor-β receptor type II transgene (18) as well as in the ischemic core after cerebral ischemia in the rat brain (59). However, reactive microglia in both groups of mice reported here had ramified thin and long cell processes and did not appear to be phagocytic based on morphological criteria (amoeboid structure, puffy cytoplasm, few or no processes resembling brain-infiltrating macrophages) (60).

DISCUSSION

Nutraceuticals are naturally occurring compounds that, because of their existence throughout evolution, tend to have fewer side effects than designer pharmaceuticals. The purpose of the present study was to evaluate the effects of TA, a plant-derived flavonoid nutraceutical, on behavioral impairment, AD-like pathology, and APP metabolism *in vivo* and *in vitro*. Collectively, our results demonstrate that oral TA prevents behavioral impairment, mitigates cerebral amyloidosis, and promotes nonamyloidogenic APP processing by inhibiting BACE1 expression and β-secretase activity without altering BACE1 mRNA abundance in an accelerated mouse model of

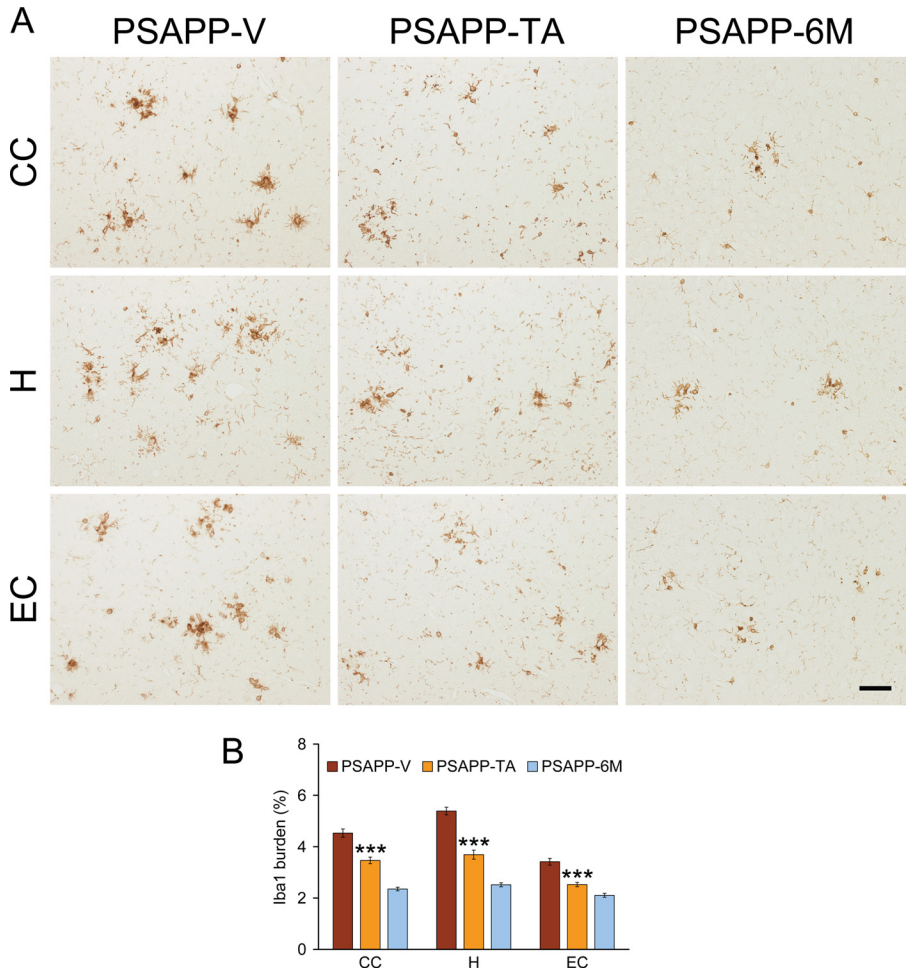

FIGURE 8. **Attenuated reactive microgliosis in PSAPP mice treated with tannic acid.** Data were obtained from PSAPP mice treated with vehicle (*PSAPP-V*, $n = 16$) or with TA (*PSAPP-TA*, $n = 16$) for 6 months commencing at 6 months of age. In addition, untreated PSAPP mice at 6 months of age (*PSAPP-6M*, $n = 12$) were included in the analysis. *A*, representative photomicrographs of Iba1 immunohistochemistry for β-amyloid plaque-associated microgliosis are shown in PSAPP-V and PSAPP-TA mice at 12 months of age as well as in PSAPP-6M mice. Brain regions shown include *CC* (*top*), *H* (*middle*), and *EC* (*bottom*). *Scale bar* denotes 50 μm. *B*, quantitative image analysis for Iba1 burden is shown for each brain region indicated on the *x* axis. All statistical comparisons are *versus* PSAPP-TA mice.

cerebral amyloid deposition. In addition, TA dose-dependently inhibited $A\beta_{1-40}$ and $A\beta_{1-42}$ production and β-CTF cleavage in human SweAPP-expressing neuron-like cells *in vitro*. Finally, TA attenuated neuroinflammation in PSAPP mice, including β-amyloid plaque-associated gliosis and expression of the pro-inflammatory cytokines TNF-α and IL-1β.

TA is a member of the tannin category of plant-derived polyphenols, and is found in numerous herbaceous and woody plants. Tannins are chemically divided into four groups based on the structure of the monomer: hydrolysable tannins, condensed tannins (proanthocyanidins), phlorotannins, and complex tannins. Among these, hydrolyzable tannins (including TA) are derivatives of gallic acid (3,4,5-trihydroxyl benzoic acid), characterized by a variable number of gallate moieties esterified to a core phenol (29). Similar to other polyphenols, tannins have antioxidant/free radical scavenging, antiviral/bacterial, anticarcinogenic, antimutagenic, and anti-inflammatory properties (29, 61–63). Given these pleiotropic biological activities, TA has yielded promising clinical results against cancer (61), myocardial infarction (64), and renal failure (65).

In this study, we orally administered TA to mice at 30 mg/kg/day via gavage, as this treatment strategy more precisely delivers the targeted amount of agent compared with *ad libitum* access in drinking water or chow. TA is well tolerated in rodents, with a lethal dose resulting in 50% mortality as high as 2,260 mg/kg in the rat (66), and the dose that we administered to mice is orders of magnitude lower. Similarly, the human tolerable daily intake of TA is 13.6 g/60 kg (67). Unwanted side effects are always a concern in the clinic, and it is important to note that we did not observe evidence for adverse events associated with TA treatment in mice, including abnormal behavior, altered body weight or food intake, or mortality. Likewise, we did not detect pathological features in major organs such as the brain, lung, heart, liver, digestive tract, and kidney upon postmortem examination of TA-treated PSAPP or WT mice. These findings reinforce the notion that the dose of TA used in our study is safe; of course, our results are limited to mice. Because BACE1 likely has important physiologic functions, and TA may have long-term toxic effects due to inhibition of BACE1, possible side effects of TA would need to be properly investigated in humans.

It is important to consider how TA exerts its biological effects. The compound is a high molecular weight molecule that does not easily penetrate the cell or freely cross the blood-

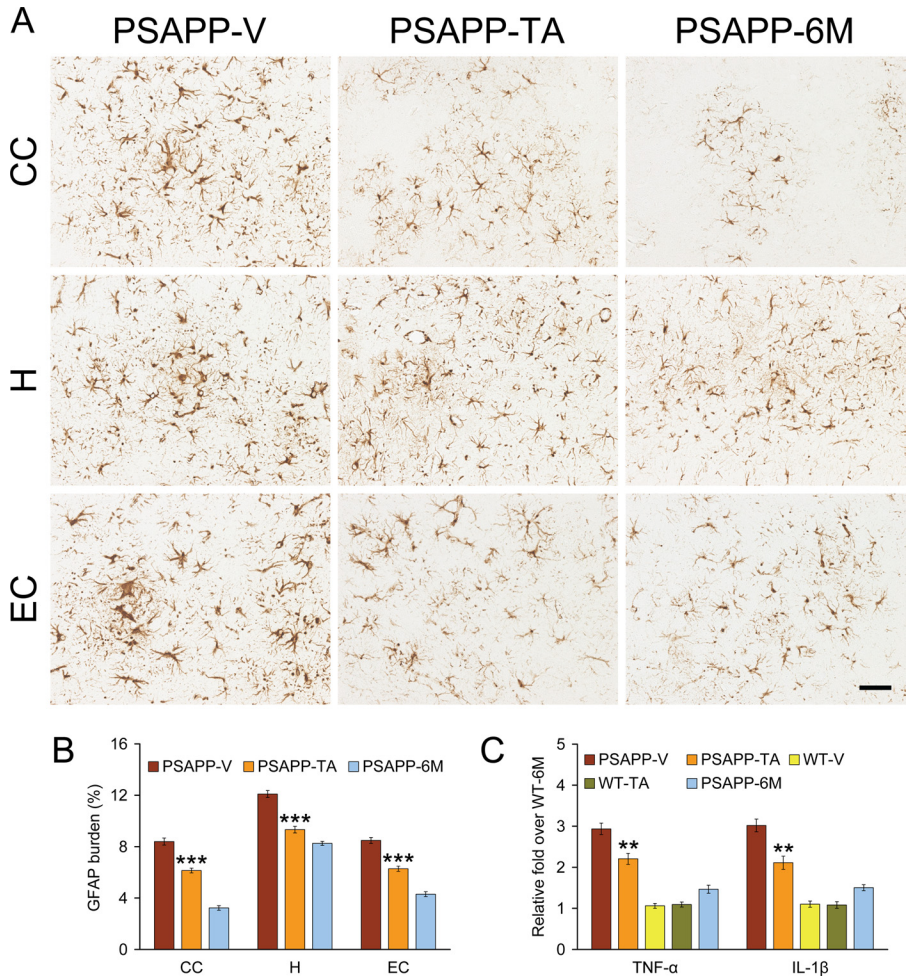

FIGURE 9. **Tannic acid-treated PSAPP mice have reduced astrocytosis.** Data for *A* and *B* were obtained from PSAPP mice treated with vehicle (*PSAPP-V*, $n = 16$) or with TA (*PSAPP-TA*, $n = 16$) for 6 months beginning at 6 months of age. In addition, 6-month-old untreated PSAPP mice (*PSAPP-6M*, $n = 12$) and wild-type (*WT-6M*, $n = 12$) mice were included for *C*. *A*, representative photomicrographs of GFAP immunohistochemistry, taken from each brain region indicated on the *left* (*CC*, *top*; *H*, *middle*; *EC*, *bottom*), for β-amyloid plaque-associated astrocytosis are shown for PSAPP-V and PSAPP-TA mice at 12 months of age and for untreated PSAPP-6M mice. *Scale bar* denotes 50 μm. *B*, quantitative image analysis for GFAP burden is shown for each brain region indicated on the *x* axis. *C*, expression of brain proinflammatory TNF-α and IL-1β cytokine mRNAs is attenuated by TA treatment in PSAPP mice. Data are expressed as relative fold over WT-6M mice, and all statistical comparisons are *versus* PSAPP-TA mice.

brain barrier. Nonetheless, TA is metabolized into much lower molecular weight, absorbable tannins that are biologically active in various organs including the brain (68). For example, hydrolysable tannins are degraded to gallic acid, pyrogallol, phloroglucinol, and finally to acetate and butyrate via sequential enzymatic action (29). In particular, oral administration of gallic acid led to intestinal absorption over a period of ~60 min in rodents (69), which equated to 76 min in humans (70). Flavonoids including gallate have also been shown to cross into the brain in rodents (68, 71, 72). Thus, the gallate moiety is a likely candidate for mediating the bioactivity of TA in our system; yet, future study is warranted to characterize which chemical structure in TA plays a pivotal role on mitigating Aβ pathology.

Our *in vivo* and *in vitro* results show that TA shifts APP metabolism toward the nonamyloidogenic pathway. Specifically, TA lowered BACE1 expression (without any change in BACE1 mRNA expression) and β-secretase activity (but had no effect on α-secretase activity), leading to reduced abundance of the amyloidogenic C99 and phospho-C99 APP CTFs, attenuated sAPP-β abundance, and lower levels of Aβ peptides. Interestingly, TA exerts its effects on BACE1 both at the post-translational level and also by directly attenuating enzymatic activity, as demonstrated in a cell-free BACE1 activity assay. Although Aβ is generally regarded as the pathogenic species in both mouse models of cerebral amyloidosis and in human AD, it remains possible that TA reduction of any combination of amyloidogenic APP metabolites may be responsible for bringing about reduced behavioral impairment in PSAPP mice.

It is generally recognized that APP is a limiting reagent in the cell, and it has been postulated that α- and β-secretases compete for APP proteolysis (73). Reduced β-secretase activity could therefore be responsible for mitigated cerebral Aβ pathology in TA-treated PSAPP mice and attenuated Aβ secretion by SweAPP N2a cells. In this regard, we previously demonstrated that another polyphenol, EGCG (a bioactive flavonoid ingredient in green tea), was also able to promote nonamyloidogenic APP metabolism in the Tg2576 cerebral amyloidosis mouse model and in SweAPP N2a cells (23). Interestingly, the mechanism for the beneficial effects of EGCG on nonamyloidogenic APP processing relied on promoting activity

of the candidate α-secretase, a disintegrin and metalloprotease 10 (23, 24). Given their complementary modes of action then, a combined TA/EGCG approach may make sense, at least in principle, as an Aβ lowering strategy.

It is generally accepted that newly produced Aβ exists in dynamic equilibrium between soluble and deposited forms in the brain, with continual transport of soluble Aβ out of the brain and into the circulation (10). In this regard, it has been reported that TA inhibits Aβ fibrillogenesis, and destabilizes preformed Aβ fibrils *in vitro* (30). We tested the impact of TA on various pools of Aβ peptides *in vivo*, and observed that TA treatment nonselectively reduced Aβ in TBS-, SDS-, and guanidine HCl-soluble brain homogenate fractions from PSAPP mice. One interesting exception was TBS-soluble $A\beta_{1-42}$, which remained unaltered by oral TA treatment. $A\beta_{1-42}$ is typically thought to have a higher propensity to form oligomers and higher molecular weight aggregates than $A\beta_{1-40}$ (11, 74), and we went on to probe whether TA impacted Aβ oligomers. Data showed a reduced abundance of both monomeric and oligomeric Aβ by Western blot and reduced Aβ oligomers by sandwich ELISA in brain homogenates from TA-treated PSAPP mice. These results may be because of a combination of reduced APP metabolism to Aβ (concentration-dependent effect on Aβ oligomer formation) and perhaps a more direct effect of TA on inhibiting assembly of structured Aβ oligomers/aggregates as has been demonstrated for both TA and EGCG (30, 75). If this were the case, then it opens the possibility of a negative feedback loop where loss of Aβ oligomers might down-regulate BACE1 activity and/or expression.

Although our *in vivo* and *in vitro* data suggest that TA has a direct effect on reducing Aβ production by neuronal cells, it remains possible *in vivo* that the compound exerts its effects on non-neuronal cell types as well. For example, TA has been reported to have antioxidant and anti-inflammatory properties (76, 77), and we went on to determine whether the compound impacted neuroinflammation, an important AD pathoetiologic hallmark (53, 54), in PSAPP mice. Interestingly, oral TA treatment reduced microgliosis, astrocytosis, and expression of the proinflammatory cytokines TNF-α and IL-1β in PSAPP mice. One interpretation of these results is that TA has an anti-inflammatory effect independent of its anti-amyloidogenic property. Yet, it is important to note that neuroinflammation and cerebral amyloid generally correlate in mouse models and in human AD (18, 42, 43, 55–57, 78). Thus, it remains possible that reduced neuroinflammation is secondary to TA amelioration of cerebral amyloidosis.

It deserves mentioning that our present findings are given added importance based on the intense β-secretase inhibition focus as an Alzheimer therapeutic approach. Unfortunately, designer drugs have yet to pan out in the clinic, and ~16 compounds have been abandoned by pharmaceutical companies, mainly due to toxicity issues in pre-clinical rodent models of the disease (alzforum.org). The present nutraceutical approach offers a new class of drug for inhibiting β-secretase with few if any side effects in PSAPP mice or in humans, and provides proof-of-concept that BACE1 is indeed still a "drug-able target."

In conclusion, our data demonstrate that the plant-derived polyphenol, TA, opposes behavioral impairment and AD-like pathology in PSAPP mice. These beneficial effects occur with reduction in: cerebral Aβ pathology, cleavage of β-CTF, sAPP-β, BACE1 protein expression and activity, and neuroinflammation. If Aβ pathology in these transgenic models is representative of the clinical syndrome, then our data raise the possibility that dietary supplementation with TA may represent a potentially safe and effective AD prophylaxis.

Acknowledgments—We thank Dr. Joshua J. Breunig for helpful discussion of the manuscript, and Dr. Gopal Thinakaran for generously gifting the SweAPP N2a cells.

REFERENCES

1. Brookmeyer, R., and Gray, S. (2000) Methods for projecting the incidence and prevalence of chronic diseases in aging populations: application to Alzheimer's disease. *Stat. Med.* **19,** 1481–1493
2. Selkoe, D. J. (2001) Alzheimer's disease: genes, proteins, and therapy. *Physiol. Rev.* **81,** 741–766
3. Rozemuller, J. M., Eikelenboom, P., Stam, F. C., Beyreuther, K., and Masters, C. L. (1989) A4 protein in Alzheimer's disease: primary and secondary cellular events in extracellular amyloid deposition. *J. Neuropathol. Exp. Neurol.* **48,** 674–691
4. Hardy, J., and Allsop, D. (1991) Amyloid deposition as the central event in the aetiology of Alzheimer's disease. *Trends Pharmacol. Sci.* **12,** 383–388
5. De Strooper, B., Saftig, P., Craessaerts, K., Vanderstichele, H., Guhde, G., Annaert, W., Von Figura, K., and Van Leuven, F. (1998) Deficiency of presenilin-1 inhibits the normal cleavage of amyloid precursor protein. *Nature* **391,** 387–390
6. Sinha, S., and Lieberburg, I. (1999) Cellular mechanisms of β-amyloid production and secretion. *Proc. Natl. Acad. Sci. U.S.A.* **96,** 11049–11053
7. Vassar, R., Bennett, B. D., Babu-Khan, S., Kahn, S., Mendiaz, E. A., Denis, P., Teplow, D.B., Ross, S., Amarante, P., Loeloff, R., Luo, Y., Fisher, S., Fuller, J., Edenson, S., Lile, J., Jarosinski, M. A., Biere, A. L., Curran, E., Burgess, T., Louis, J. C., Collins, F., Treanor, J., Rogers, G., and Citron, M. (1999) β-Secretase cleavage of Alzheimer's amyloid precursor protein by the transmembrane aspartic protease BACE. *Science* **286,** 735–741
8. Vassar, R., Kovacs, D. M., Yan, R., and Wong, P. C. (2009) The β-secretase enzyme BACE in health and Alzheimer's disease: regulation, cell biology, function, and therapeutic potential. *J. Neurosci.* **29,** 12787–12794
9. Yan, R., Bienkowski, M. J., Shuck, M. E., Miao, H., Tory, M. C., Pauley, A. M., Brashier, J. R., Stratman, N. C., Mathews, W. R., Buhl, A. E., Carter, D. B., Tomasselli, A. G., Parodi, L. A., Heinrikson, R. L., and Gurney, M. E. (1999) Membrane-anchored aspartyl protease with Alzheimer's disease β-secretase activity. *Nature* **402,** 533–537
10. DeMattos, R. B., Bales, K. R., Cummins, D. J., Paul, S. M., and Holtzman, D. M. (2002) Brain to plasma amyloid-β efflux: a measure of brain amyloid burden in a mouse model of Alzheimer's disease. *Science* **295,** 2264–2267
11. Walsh, D. M., Klyubin, I., Fadeeva, J. V., Cullen, W. K., Anwyl, R., Wolfe, M. S., Rowan, M. J., and Selkoe, D. J. (2002) Naturally secreted oligomers of amyloid β protein potently inhibit hippocampal long-term potentiation *in vivo*. *Nature* **416,** 535–539
12. Cleary, J. P., Walsh, D. M., Hofmeister, J. J., Shankar, G. M., Kuskowski, M. A., Selkoe, D. J., and Ashe, K. H. (2005) Natural oligomers of the amyloid-β protein specifically disrupt cognitive function. *Nat. Neurosci.* **8,** 79–84
13. Shankar, G. M., Li, S., Mehta, T. H., Garcia-Munoz, A., Shepardson, N. E., Smith, I., Brett, F. M., Farrell, M. A., Rowan, M. J., Lemere, C. A., Regan, C. M., Walsh, D. M., Sabatini, B. L., and Selkoe, D. J. (2008) Amyloid-β protein dimers isolated directly from Alzheimer's brains impair synaptic plasticity and memory. *Nat. Med.* **14,** 837–842
14. Schenk, D., Barbour, R., Dunn, W., Gordon, G., Grajeda, H., Guido, T., Hu, K., Huang, J., Johnson-Wood, K., Khan, K., Kholodenko, D., Lee, M., Liao, Z., Lieberburg, I., Motter, R., Mutter, L., Soriano, F., Shopp, G., Vasquez,

N., Vandevert, C., Walker, S., Wogulis, M., Yednock, T., Games, D., and Seubert, P. (1999) Immunization with amyloid-β attenuates Alzheimer-disease-like pathology in the PDAPP mouse. *Nature* **400,** 173–177
15. Weggen, S., Eriksen, J. L., Das, P., Sagi, S. A., Wang, R., Pietrzik, C. U., Findlay, K. A., Smith, T. E., Murphy, M. P., Bulter, T., Kang, D. E., Marquez-Sterling, N., Golde, T. E., and Koo, E. H. (2001) A subset of NSAIDs lower amyloidogenic Aβ42 independently of cyclooxygenase activity. *Nature* **414,** 212–216
16. Tan, J., Town, T., Crawford, F., Mori, T., DelleDonne, A., Crescentini, R., Obregon, D., Flavell, R. A., and Mullan, M. J. (2002) Role of CD40 ligand in amyloidosis in transgenic Alzheimer's mice. *Nat. Neurosci.* **5,** 1288–1293
17. Kukar, T. L., Ladd, T. B., Bann, M. A., Fraering, P. C., Narlawar, R., Maharvi, G. M., Healy, B., Chapman, R., Welzel, A. T., Price, R. W., Moore, B., Rangachari, V., Cusack, B., Eriksen, J., Jansen-West, K., Verbeeck, C., Yager, D., Eckman, C., Ye, W., Sagi, S., Cottrell, B. A., Torpey, J., Rosenberry, T. L., Fauq, A., Wolfe, M. S., Schmidt, B., Walsh, D. M., Koo, E. H., and Golde, T. E. (2008) Substrate-targeting γ-secretase modulators. *Nature* **453,** 925–929
18. Town, T., Laouar, Y., Pittenger, C., Mori, T., Szekely, C.A., Tan, J., Duman, R. S., and Flavell, R. A. (2008) Blocking TGF-β-Smad2/3 innate immune signaling mitigates Alzheimer-like pathology. *Nat. Med.* **14,** 681–687
19. Zhu, Y., Hou, H., Rezai-Zadeh, K., Giunta, B., Ruscin, A., Gemma, C., Jin, J., Dragicevic, N., Bradshaw, P., Rasool, S., Glabe, C. G., Ehrhart, J., Bickford, P., Mori, T., Obregon, D., Town, T., and Tan, J. (2011) CD45 deficiency drives amyloid-β peptide oligomers and neuronal loss in Alzheimer's disease mice. *J. Neurosci.* **31,** 1355–1365
20. Breitner, J., Evans, D., Lyketsos, C., Martin, B., and Meinert, C. (2007) ADAPT trial data. *Am. J. Med.* **120,** e3
21. Montine, T. J., Sonnen, J. A., Milne, G., Baker, L. D., and Breitner, J. C. (2010) Elevated ratio of urinary metabolites of thromboxane and prostacyclin is associated with adverse cardiovascular events in ADAPT. *PLoS One* **5,** e9340
22. Georgiou, N. A., Garssen, J., and Witkamp, R. F. (2011) Pharma-nutrition interface: the gap is narrowing. *Eur. J. Pharmacol.* **651,** 1–8
23. Rezai-Zadeh, K., Shytle, D., Sun, N., Mori, T., Hou, H., Jeanniton, D., Ehrhart, J., Townsend, K., Zeng, J., Morgan, D., Hardy, J., Town, T., and Tan, J. (2005) Green tea epigallocatechin-3-gallate (EGCG) modulates amyloid precursor protein cleavage and reduces cerebral amyloidosis in Alzheimer transgenic mice. *J. Neurosci.* **25,** 8807–8814
24. Obregon, D. F., Rezai-Zadeh, K., Bai, Y., Sun, N., Hou, H., Ehrhart, J., Zeng, J., Mori, T., Arendash, G. W., Shytle, D., Town, T., and Tan, J. (2006) ADAM10 activation is required for green tea (−)-epigallocatechin-3-gallate-induced α-secretase cleavage of amyloid precursor protein. *J. Biol. Chem.* **281,** 16419–16427
25. Rezai-Zadeh, K., Douglas Shytle, R., Bai, Y., Tian, J., Hou, H., Mori, T., Zeng, J., Obregon, D., Town, T., and Tan, J. (2009) Flavonoid-mediated presenilin-1 phosphorylation reduces Alzheimer's disease β-amyloid production. *J. Cell Mol. Med.* **13,** 574–588
26. Ono, K., Yoshiike, Y., Takashima, A., Hasegawa, K., Naiki, H., and Yamada, M. (2003) Potent anti-amyloidogenic and fibril-destabilizing effects of polyphenols *in vitro*: implications for the prevention and therapeutics of Alzheimer's disease. *J. Neurochem.* **87,** 172–181
27. Marambaud, P., Zhao, H., and Davies, P. (2005) Resveratrol promotes clearance of Alzheimer's disease amyloid-β peptides. *J. Biol. Chem.* **280,** 37377–37382
28. Arendash, G. W., Mori, T., Cao, C., Mamcarz, M., Runfeldt, M., Dickson, A., Rezai-Zadeh, K., Tan, J., Citron, B. A., Lin, X., Echeverria, V., and Potter, H. (2009) Caffeine reverses cognitive impairment and decreases brain amyloid-β levels in aged Alzheimer's disease mice. *J. Alzheimers Dis.* **17,** 661–680
29. Serrano, J., Puupponen-Pimiä, R., Dauer, A., Aura, A. M., and Saura-Calixto, F. (2009) Tannins: current knowledge of food sources, intake, bioavailability and biological effects. *Mol. Nutr. Food Res.* **53,** S310–S329
30. Ono, K., Hasegawa, K., Naiki, H., and Yamada, M. (2004) Anti-amyloidogenic activity of tannic acid and its activity to destabilize Alzheimer's β-amyloid fibrils *in vitro*. *Biochim. Biophys. Acta* **1690,** 193–202
31. Ehrnhoefer, D. E., Bieschke, J., Boeddrich, A., Herbst, M., Masino, L., Lurz, R., Engemann, S., Pastore, A., and Wanker, E. E. (2008) EGCG redirects amyloidogenic polypeptides into unstructured, off-pathway oligomers. *Nat. Struct. Mol. Biol.* **15,** 558–566
32. Meng, F., Abedini, A., Plesner, A., Verchere, C. B., and Raleigh, D. P. (2010) The flavanol (−)-epigallocatechin 3-gallate inhibits amyloid formation by islet amyloid polypeptide, disaggregates amyloid fibrils, and protects cultured cells against IAPP-induced toxicity. *Biochemistry* **49,** 8127–8133
33. Borchelt, D. R., Ratovitski, T., van Lare, J., Lee, M. K., Gonzales, V., Jenkins, N. A., Copeland, N. G., Price, D. L., and Sisodia, S. S. (1997) Accelerated amyloid deposition in the brains of transgenic mice coexpressing mutant presenilin 1 and amyloid precursor proteins. *Neuron* **19,** 939–945
34. Arendash, G. W., King, D. L., Gordon, M. N., Morgan, D., Hatcher, J. M., Hope, C. E., and Diamond, D. M. (2001) Progressive, age-related behavioral impairments in transgenic mice carrying both mutant amyloid precursor protein and presenilin-1 transgenes. *Brain Res.* **891,** 42–53
35. Jankowsky, J. L., Slunt, H. H., Gonzales, V., Jenkins, N. A., Copeland, N. G., and Borchelt, D. R. (2004) APP processing and amyloid deposition in mice haplo-insufficient for presenilin 1. *Neurobiol. Aging* **25,** 885–892
36. Garcia-Alloza, M., Robbins, E. M., Zhang-Nunes, S. X., Purcell, S. M., Betensky, R. A., Raju, S., Prada, C., Greenberg, S. M., Bacskai, B. J., and Frosch, M. P. (2006) Characterization of amyloid deposition in the APPswe/PS1dE9 mouse model of Alzheimer disease. *Neurobiol. Dis.* **24,** 516–524
37. Laghmouch, A., Bertholet, J. Y., and Crusio, W. E. (1997) Hippocampal morphology and open-field behavior in *Mus musculus domesticus* and *Mus spretus* inbred mice. *Behav. Genet.* **27,** 67–73
38. Kim, K. S., and Han, P. L. (2006) Optimization of chronic stress paradigms using anxiety- and depression-like behavioral parameters. *J. Neurosci. Res.* **83,** 497–507
39. De Rosa, R., Garcia, A. A., Braschi, C., Capsoni, S., Maffei, L., Berardi, N., and Cattaneo, A. (2005) Intranasal administration of nerve growth factor (NGF) rescues recognition memory deficits in AD11 anti-NGF transgenic mice. *Proc. Natl. Acad. Sci. U.S.A.* **102,** 3811–3816
40. Morris, R.G., Garrud, P., Rawlins, J. N., and O'Keefe, J. (1982) Place navigation impaired in rats with hippocampal lesions. *Nature* **297,** 681–683
41. Good, M., and Honey, R. C. (1997) Dissociable effects of selective lesions to hippocampal subsystems on exploratory behavior, contextual learning, and spatial learning. *Behav. Neurosci.* **111,** 487–493
42. Mori, T., Town, T., Tan, J., Yada, N., Horikoshi, Y., Yamamoto, J., Shimoda, T., Kamanaka, Y., Tateishi, N., and Asano, T. (2006) Arundic acid ameliorates cerebral amyloidosis and gliosis in Alzheimer transgenic mice. *J. Pharmacol. Exp. Ther.* **318,** 571–578
43. Mori, T., Koyama, N., Arendash, G. W., Horikoshi-Sakuraba, Y., Tan, J., and Town, T. (2010) Overexpression of human S100B exacerbates cerebral amyloidosis and gliosis in the Tg2576 mouse model of Alzheimer's disease. *Glia* **58,** 300–314
44. Franklin, K. B. J., and Paxinos, G. (2001) *The Mouse Brain in Stereotaxic Coordinates*, Academic Press, San Diego, CA
45. Tan, J., Town, T., Mori, T., Wu, Y., Saxe, M., Crawford, F., and Mullan, M. (2000) CD45 opposes β-amyloid peptide-induced microglial activation via inhibition of p44/42 mitogen-activated protein kinase. *J. Neurosci.* **20,** 7587–7594
46. Kawarabayashi, T., Younkin, L. H., Saido, T. C., Shoji, M., Ashe, K. H., and Younkin, S. G. (2001) Age-dependent changes in brain, CSF, and plasma amyloid β protein in the Tg2576 transgenic mouse model of Alzheimer's disease. *J. Neurosci.* **21,** 372–381
47. Jankowsky, J. L., Slunt, H. H., Gonzales, V., Savonenko, A. V., Wen, J. C., Jenkins, N. A., Copeland, N. G., Younkin, L. H., Lester, H. A., Younkin, S. G., and Borchelt, D. R. (2005) Persistent amyloidosis following suppression of Aβ production in a transgenic model of Alzheimer disease. *PLoS Med.* **2,** e355
48. Horikoshi, Y., Sakaguchi, G., Becker, A. G., Gray, A. J., Duff, K., Aisen, P. S., Yamaguchi, H., Maeda, M., Kinoshita, N., and Matsuoka, Y. (2004) Development of Aβ terminal end-specific antibodies and sensitive ELISA for Aβ variant. *Biochem. Biophys. Res. Commun.* **319,** 733–737
49. Xia, W., Yang, T., Shankar, G., Smith, I. M., Shen, Y., Walsh, D. M., and Selkoe, D. J. (2009) A specific enzyme-linked immunosorbent assay for measuring β-amyloid protein oligomers in human plasma and brain tissue of patients with Alzheimer disease. *Arch. Neurol.* **66,** 190–199

50. Monney, L., Sabatos, C. A., Gaglia, J. L., Ryu, A., Waldner, H., Chernova, T., Manning, S., Greenfield, E. A., Coyle, A. J., Sobel, R. A., Freeman, G. J., and Kuchroo, V. K. (2002) Th1-specific cell surface protein Tim-3 regulates macrophage activation and severity of an autoimmune disease. *Nature* **415,** 536–541
51. King, D. L., Arendash, G. W., Crawford, F., Sterk, T., Menendez, J., and Mullan, M. J. (1999) Progressive and gender-dependent cognitive impairment in the APP_{sw} transgenic mouse model for Alzheimer's disease. *Behav. Brain Res.* **103,** 145–162
52. Ellis, R. J., Olichney, J. M., Thal, L. J., Mirra, S. S., Morris, J. C., Beekly, D., and Heyman, A. (1996) Cerebral amyloid angiopathy in the brains of patients with Alzheimer's disease: the CERAD experience, Part XV. *Neurology* **46,** 1592–1596
53. Griffin, W. S., Sheng, J. G., Royston, M. C., Gentleman, S. M., McKenzie, J. E., Graham, D. I., Roberts, G. W., and Mrak, R. E. (1998) Glial-neuronal interactions in Alzheimer's disease: the potential role of a 'cytokine cycle' in disease progression. *Brain Pathol.* **8,** 65–72
54. Akiyama, H., Barger, S., Barnum, S., Bradt, B., Bauer, J., Cole, G. M., Cooper, N. R., Eikelenboom, P., Emmerling, M., Fiebich, B. L., Finch, C. E., Frautschy, S., Griffin, W. S., Hampel, H., Hull, M., Landreth, G., Lue, L., Mrak, R., Mackenzie, I. R., McGeer, P. L., O'Banion, M. K., Pachter, J., Pasinetti, G., Plata-Salaman, C., Rogers, J., Rydel, R., Shen, Y., Streit, W., Strohmeyer, R., Tooyoma, I., Van Muiswinkel, F. L., Veerhuis, R., Walker, D., Webster, S., Wegrzyniak, B., Wenk, G., and Wyss-Coray, T. (2000) Inflammation and Alzheimer's disease. *Neurobiol. Aging* **21,** 383–421
55. Benzing, W. C., Wujek, J. R., Ward, E. K., Shaffer, D., Ashe, K. H., Younkin, S. G., and Brunden, K. R. (1999) Evidence for glial-mediated inflammation in aged APP_{sw} transgenic mice. *Neurobiol. Aging* **20,** 581–589
56. Stalder, M., Phinney, A., Probst, A., Sommer, B., Staufenbiel, M., and Jucker, M. (1999) Association of microglia with amyloid plaques in brains of APP23 transgenic mice. *Am. J. Pathol.* **154,** 1673–1684
57. Lim, G. P., Yang, F., Chu, T., Chen, P., Beech, W., Teter, B., Tran, T., Ubeda, O., Ashe, K. H., Frautschy, S. A., and Cole, G. M. (2000) Ibuprofen suppresses plaque pathology and inflammation in a mouse model for Alzheimer's disease. *J. Neurosci.* **20,** 5709–5714
58. Stalder, A. K., Ermini, F., Bondolfi, L., Krenger, W., Burbach, G. J., Deller, T., Coomaraswamy, J., Staufenbiel, M., Landmann, R., and Jucker, M. (2005) Invasion of hematopoietic cells into the brain of amyloid precursor protein transgenic mice. *J. Neurosci.* **25,** 11125–11132
59. Ito, D., Tanaka, K., Suzuki, S., Dembo, T., and Fukuuchi, Y. (2001) Enhanced expression of Iba1, ionized calcium-binding adapter molecule 1, after transient focal cerebral ischemia in rat brain. *Stroke* **32,** 1208–1215
60. Streit, W. J. (2005) in *Neuroglia* (Kettermann, H., and Ransom, B. R., eds) pp. 60–71, Oxford University Press, New York
61. Nepka, C., Sivridis, E., Antonoglou, O., Kortsaris, A., Georgellis, A., Taitzoglou, I., Hytiroglou, P., Papadimitriou, C., Zintzaras, I., and Kouretas, D. (1999) Chemopreventive activity of very low dose dietary tannic acid administration in hepatoma bearing C3H male mice. *Cancer Lett.* **141,** 57–62
62. Chen, S. C., and Chung, K. T. (2000) Mutagenicity and antimutagenicity studies of tannic acid and its related compounds. *Food Chem. Toxicol.* **38,** 1–5
63. Andrade, R. G., Jr., Dalvi, L. T., Silva, J. M., Jr., Lopes, G. K., Alonso, A., and Hermes-Lima, M. (2005) The antioxidant effect of tannic acid on the *in vitro* copper-mediated formation of free radicals. *Arch. Biochem. Biophys.* **437,** 1–9
64. Zhang, H., Zhu, S. J., Wang, D., Wei, Y. J., and Hu, S. S. (2009) Intramyocardial injection of tannic acid attenuates postinfarction remodeling: a novel approach to stabilize the breaking extracellular matrix. *J. Thorac. Cardiovasc. Surg.* **137,** 216–222, 222e1–2
65. Yokozawa, T., Fujioka, K., Oura, H., Nonaka, G., and Nishioka, I. (1991) Effects of rhubarb tannins on uremic toxins. *Nephron* **58,** 155–160
66. Boyd, E. M., Bereczky, K., and Godi, I. (1965) The acute toxicity of tannic acid administered intragastrically. *Can. Med. Assoc. J.* **92,** 1292–1297
67. Bian, Y., Masuda, A., Matsuura, T., Ito, M., Okushin, K., Engel, A. G., and Ohno, K. (2009) Tannic acid facilitates expression of the polypyrimidine tract binding protein and alleviates deleterious inclusion of CHRNA1 exon P3A due to an hnRNP H-disrupting mutation in congenital myasthenic syndrome. *Hum. Mol. Genet.* **18,** 1229–1237
68. Medić-Sarić, M., Rastija, V., Bojić, M., and Males, Z. (2009) From functional food to medicinal product: systematic approach in analysis of polyphenolics from propolis and wine. *Nutr. J.* **8,** 33
69. Konishi, Y., Hitomi, Y., and Yoshioka, E. (2004) Intestinal absorption of *p*-coumaric and gallic acids in rats after oral administration. *J. Agric. Food Chem.* **52,** 2527–2532
70. Shahrzad, S., Aoyagi, K., Winter, A., Koyama, A., and Bitsch, I. (2001) Pharmacokinetics of gallic acid and its relative bioavailability from tea in healthy humans. *J. Nutr.* **131,** 1207–1210
71. Mandel, S., Amit, T., Reznichenko, L., Weinreb, O., and Youdim, M. B. (2006) Green tea catechins as brain-permeable, natural iron chelators-antioxidants for the treatment of neurodegenerative disorders. *Mol. Nutr. Food Res.* **50,** 229–234
72. Ferruzzi, M. G., Lobo, J. K., Janle, E. M., Cooper, B., Simon, J. E., Wu, Q. L., Welch, C., Ho, L., Weaver, C., and Pasinetti, G. M. (2009) Bioavailability of gallic acid and catechins from grape seed polyphenol extract is improved by repeated dosing in rats: implications for treatment in Alzheimer's disease. *J. Alzheimers's Dis.* **18,** 113–124
73. Gandhi, S., Refolo, L. M., and Sambamurti, K. (2004) Amyloid precursor protein compartmentalization restricts β-amyloid production: therapeutic targets based on BACE compartmentalization. *J. Mol. Neurosci.* **24,** 137–143
74. Lesné, S., Koh, M. T., Kotilinek, L., Kayed, R., Glabe, C. G., Yang, A., Gallagher, M., and Ashe, K.H. (2006) A specific amyloid-β protein assembly in the brain impairs memory. *Nature* **440,** 352–357
75. Bieschke, J., Russ, J., Friedrich, R. P., Ehrnhoefer, D.E., Wobst, H., Neugebauer, K., and Wanker, E. E. (2010) EGCG remodels mature α-synuclein and amyloid-β fibrils and reduces cellular toxicity. *Proc. Natl. Acad. Sci. U.S.A.* **107,** 7710–7715
76. Gali, H. U., Perchellet, E. M., Klish, D. S., Johnson, J. M., and Perchellet, J. P. (1992) Hydrolyzable tannins: potent inhibitors of hydroperoxide production and tumor promotion in mouse skin treated with 12-*O*-tetradecanoylphorbol-13-acetate *in vivo*. *Int. J. Cancer* **51,** 425–432
77. Sehrawat, A., Sharma, S., and Sultana, S. (2006) Preventive effect of tannic acid on 2-acetylaminofluorene induced antioxidant level, tumor promotion and hepatotoxicity: a chemopreventive study. *Redox Rep.* **11,** 85–95
78. McGeer, P. L., Itagaki, S., Tago, H., and McGeer, E. G. (1987) Reactive microglia in patients with senile dementia of the Alzheimer type are positive for the histocompatibility glycoprotein HLA-DR. *Neurosci. Lett.* **79,** 195–200